J. Fluid Mech. (2008), *vol.* 616, *pp.* 357–395. © 2008 Cambridge University Press
doi:10.1017/S0022112008003820 Printed in the United Kingdom

Lagrangian stochastic models for turbulent relative dispersion based on particle pair rotation

GIANNI PAGNINI†

ISAC-CNR, via Gobetti 101, I-40129 Bologna, Italy

(Received 2 May 2006 and in revised form 8 August 2008)

The physical picture of a fluid particle pair as a couple of material points rotating around their centre of mass is proposed to model turbulent relative dispersion in the inertial range. This scheme is used to constrain the non-uniqueness problem associated to the Lagrangian models in the well-mixed class and the properties of the stochastic process derived are analysed with respect to some turbulent velocity characteristics. A simple illustrative Markov model is developed in stationary homogeneous isotropic turbulence and the particle separation statistics are compared with direct numerical simulation data. In spite of the simplicity of the model, a consistent comparison is observed in the inertial range, supporting the formulation proposed.

1. Introduction

The strong efficiency of turbulent mixing makes turbulent dispersion important in environmental problems and also fundamental to understanding the nature of turbulence.

In particular, the relative dispersion between two fluid particles can be seen as the Lagrangian counterpart of the two-point velocity difference in the Eulerian theory and the results of the Eulerian theory can be applied directly, i.e. in terms of the two-point separation without any adjustment or additional assumptions. However, two-particle dispersion is not determined by Eulerian two-point statistics alone, since also Lagrangian time scales have an influence on the process.

At infinite Reynolds numbers, the particle acceleration can be considered local in time and space and thus, in the inertial range, an uncorrelated random forcing can be assumed (see Monin & Yaglom 1975, pp. 370–371, Borgas & Sawford 1991). This suggests the suitability of modelling turbulent dispersion as a first-order Markov process, even if the Markovian assumption cannot be derived from the equations of motion. Markovianity can be assumed for the relative dispersion, too. Turbulent relative dispersion with particular attention to its stochastic modelling is reviewed by Sawford (2001).

A valid application of the stochastic-model approach for describing Lagrangian statistics in turbulent flow can be found in Borgas & Yeung (2004). These authors show that stochastic models, when properly formulated, are efficient representations of the turbulent dispersion process. Moreover, in the viscous range, where the Markovian assumption is unphysical, non-Markovian corrections can be introduced (see Heppe 1998).

† Present address: ENEA, Via Martiri di Monte Sole 4, I-40129 Bologna, Italy.

https://doi.org/10.1017/S0022112008003820 Published online by Cambridge University Press

As shown by Sawford & Borgas (1994), a description of the turbulent dispersion consistent with the Kolmogorov theory (K41) (Monin & Yaglom 1971, 1975) requires the stochastic process to be continuous, i.e. it requires the formalism of the Langevin and Fokker–Planck equations (see Risken 1989; Gardiner 1990). Here, three-dimensional stationary homogeneous isotropic turbulence is considered. Let $\boldsymbol{r}(t) = \boldsymbol{r}^{(1)}(t) - \boldsymbol{r}^{(2)}(t)$ and $\boldsymbol{u}(t) = \boldsymbol{u}^{(1)}(t) - \boldsymbol{u}^{(2)}(t)$ be the three-dimensional particle separation and velocity difference vectors at time t, respectively. Then, the relative motion between two fluid particles is described by the stochastic differential equations

$$\mathrm{d}\boldsymbol{r} = \boldsymbol{u}\,\mathrm{d}t, \quad \mathrm{d}\boldsymbol{u} = \boldsymbol{a}\,\mathrm{d}t + \sqrt{2C_0\varepsilon}\,\mathrm{d}\boldsymbol{W}, \tag{1.1a,b}$$

where $\boldsymbol{a} = \boldsymbol{a}(\boldsymbol{u}, \boldsymbol{r}, t)$ is the drift term, $\sqrt{2C_0\varepsilon}$ is the noise amplitude and $\mathrm{d}\boldsymbol{W}$ is a Wiener process with zero mean and variance $\mathrm{d}t$, $\langle \mathrm{d}W_i(t)\,\mathrm{d}W_j(s)\rangle = \delta_{ij}\,\mathrm{d}t\delta(t-s)$. The noise amplitude is chosen consistently with the second-order Lagrangian structure function in K41, i.e. $S_L = \langle (u_i^{(j)}(0) - u_i^{(j)}(t))^2\rangle = C_0\varepsilon t$, $j = 1, 2$, $i = 1, 2, 3$, where C_0 is a universal constant and ε the mean rate of turbulent kinetic energy dissipation. From the theory of stochastic methods, it is known that the Lagrangian probability density function (PDF) $p_L(\boldsymbol{u}, \boldsymbol{r}; t|\boldsymbol{r}_0)$ evolves according to the Fokker–Planck equation (Risken 1989; Gardiner 1990)

$$\frac{\partial p_L}{\partial t} = -\frac{\partial}{\partial r_i}(u_i p_L) - \frac{\partial}{\partial u_i}(a_i p_L) + C_0\varepsilon\frac{\partial^2 p_L}{\partial u_i \partial u_i}. \tag{1.2}$$

In order to derive an exact, statistically founded, formulation, Thomson (1987) defined the constraint called the well-mixed condition which recovers the important physical requirement that the Eulerian and Lagrangian statistics generated by the model must be consistent, e.g. if an initially well-mixed scalar field (for constant density flows) is considered, the Lagrangian evolution of the process does not produce mean concentration gradient or concentration fluctuations. This constraint was subsequently applied also in relative dispersion (Thomson 1990). A similar work was published by Novikov (1986). The well-mixed condition is derived by applying to the Fokker–Planck equation (1.2) the following Thomson–Novikov formula (Novikov 1986; Thomson 1987)

$$p_E(\boldsymbol{u}; t|\boldsymbol{r}) = \int p_L(\boldsymbol{u}, \boldsymbol{r}; t|\boldsymbol{r}_0)\,\mathrm{d}\boldsymbol{r}_0, \tag{1.3}$$

with the initial condition $p_L(\boldsymbol{u}, \boldsymbol{r}; 0|\boldsymbol{r}_0) = \delta(\boldsymbol{r} - \boldsymbol{r}_0)p_E(\boldsymbol{u}; 0|\boldsymbol{r})$. As a consequence, the following determination of the drift term is obtained

$$a_i\, p_E = C_0\varepsilon\frac{\partial p_E}{\partial u_i} + \Phi_i, \quad \frac{\partial \Phi_i}{\partial u_i} = -\frac{\partial p_E}{\partial t} - \frac{\partial u_i p_E}{\partial r_i}, \tag{1.4}$$

where p_E is the Eulerian PDF and $|\boldsymbol{\Phi}| \to 0$ when $|\boldsymbol{u}| \to \infty$.

However, for a given Eulerian PDF, the drift coefficient $\boldsymbol{a}$ defined in (1.4) is determined up to an additive term with zero divergence with respect to $\boldsymbol{u}$. This drift indetermination, also referred to as the non-uniqueness problem, motivates the present paper. Here, a consistent formalism without indetermination is derived in the well-mixed approach, uniquely relating the drift term with a kinematical formula for relative acceleration, under the Markovian assumption. In particular, the derived closure uses the fact that turbulent flows are rotational.

This paper describes a Lagrangian stochastic model for the relative dispersion of particle pairs in stationary isotropic turbulence. The key idea is to treat the fluid particle pair as a couple of material points rotating around their centre of mass for

https://doi.org/10.1017/S0022112008003820 Published online by Cambridge University Press

turbulent relative dispersion when the particle separation falls in the inertial range. Since in the centre-of-mass reference frame the particles move only radially, it is possible to derive formulae for relative velocity and relative acceleration, thereby constraining the non-uniqueness problem.

The remainder of the paper is organized as follows. In § 2, a literature survey of the non-uniqueness problem is given, and in § 3 a closure for Lagrangian stochastic models of turbulent relative dispersion is proposed. In § 4, the properties of the new closure are investigated with respect to some fundamental aspects of fluid dynamics. In § 5, a Markovian model is formulated and compared first with data obtained from the direct numerical simulation (DNS) by Biferale *et al.* (2005) and later with other models. Finally, in § 6, the results are discussed and the conclusions are given.

2. Background to the non-uniqueness problem

In one-particle models, the non-uniqueness problem is solved in homogeneous and isotropic turbulence or in the one-dimensional case, while in two-particle models the non-uniqueness remains in the multidimensional case even in a steady homogeneous isotropic flow (Borgas & Sawford 1994). This indetermination arises because (1.3) defines a purely statistical condition and the Eulerian PDF alone does not include all the dynamical contents of the physical process.

This indetermination is a relevant problem in the improvement of Lagrangian stochastic models because solutions to (1.4) differ strongly (Borgas & Sawford 1994; Borgas, Flesch & Sawford 1997). In absolute dispersion, several selection criteria have been proposed. For example, the rotation of the particle trajectories (Wilson & Flesch 1997; Reynolds 1998, 1999*a*; Sawford 1999), the correspondence with the second-moment closures of the Reynolds-stress and scalar-flux equations (Reynolds 2002), and also the ability to represent DNS statistics was tested as a discriminator between models (Sawford & Yeung 2000, 2001). However, none of the above criteria is sufficient to define a unique model yet.

In relative dispersion, the optimal reduction to the known one-particle statistics was adopted as a selection criterion, the so-called two-to-one reduction (Borgas & Sawford 1994). However, these statistics are not adequately modelled by every model (Thomson 1990). An alternative to the non-unique well-mixed approach, which requires also the choice of an Eulerian PDF, is the moments approximation method (Kaplan & Dinar 1993). With the moments approximation method, the non-uniqueness problem is solved operationally by choosing a polynomial form for the drift term whose coefficients are determined by imposing the consistency with some Eulerian statistical moments (Pedrizzetti & Novikov 1994; Heppe 1998; Pedrizzetti 1999). However, stochastic models based on the moments approximation approach in general do not satisfy the well-mixed condition (Du, Wilson & Yee 1994). A more conclusive result is desirable.

Kurbanmuradov & Sabelfeld (1995) introduced a new approach. They considered isotropic turbulence where the relative dispersion is spatially characterized only by the modulus of the particle separation $r = (\boldsymbol{r}\cdot\boldsymbol{r})^{1/2}$ and subsequently rewrote the well-mixed models in the spherical reference frame defined by r. This reference system is the natural one for applying the two-point Eulerian theory (Monin & Yaglom 1975) in relative dispersion, in fact the line joining the two points is $\boldsymbol{r}$. This spherical reference frame was used for absolute dispersion models in two and three dimensions (Flesch & Wilson 1992; Monti & Leuzzi 1996). The new reference frame is defined by the change of variables $\{\boldsymbol{u}\} \rightarrow \{u_\parallel, u'_\perp, u''_\perp\} \rightarrow \{u_\parallel, u_\perp, \alpha\}$ where $u_\parallel = \boldsymbol{u}\cdot\boldsymbol{r}/r$,

https://doi.org/10.1017/S0022112008003820 Published online by Cambridge University Press

$u_\perp^2 = \boldsymbol{u}\cdot\boldsymbol{u} - u_\parallel^2$ and $\alpha \in [0;2\pi]$ is a uniformly distributed angle. In this frame, the two-to-one reduction is meaningless. In the new reference frame, the stochastic equations of the relative motion between two fluid particles become

$$\mathrm{d}r = u_\parallel\,\mathrm{d}t, \quad \mathrm{d}u_\parallel = \chi_\parallel\,\mathrm{d}t + \sqrt{2C_0\varepsilon}\,\mathrm{d}W_\parallel, \quad \mathrm{d}u_\perp = \chi_\perp\,\mathrm{d}t + \sqrt{2C_0\varepsilon}\,\mathrm{d}W_\perp, \quad (2.1a\text{–}c)$$

where the drift term indeterminacy remains.

This indeterminacy can be avoided by choosing to develop a stochastic process for $\{r, u_\parallel\}$, where essentially an average is taken over $u_\perp$ (see Sawford, Yeung & Borgas 2005; Sawford 2006). However, Kurbanmuradov (1997) proposed to solve the indeterminacy assuming that the longitudinal drift term $\chi_\parallel$ depends solely on the longitudinal component of the velocity and not on the orthogonal ones: $\chi_\parallel = \chi_\parallel(u_\parallel, r, t)$; here, this is called quasi-one-dimensional assumption. This assumption implies considering only the first two equations in (2.1*a–c*) and the formal reduction to a one-dimensional problem. Subsequently, the quasi-one-dimensional approach developed by Kurbanmuradov (1997) was applied by him and collaborators (Sabelfeld & Kurbanmuradov 1997, 1998; Kurbanmuradov *et al.* 1997, 2001) and by others (Borgas & Yeung 1998, 2004; Reynolds 1999*b*, Franzese & Borgas 2002). However, this class of models shows a high rate of separation (Kurbanmuradov *et al.* 2001) and a new closure is required. In the next section, a new closure is proposed starting from the fact that rotation reduces the dispersion (Borgas *et al.* 1997).

3. A closure for Lagrangian stochastic models of turbulent relative dispersion

3.1. *Lagrangian relative kinematics*

Turbulent flows are characterized by high levels of fluctuating vorticity and this plays a key role in turbulent dynamics (see Tennekes & Lumley 1972). In order to describe relative dispersion, the importance of particle rotation must be kept in mind. The simple physical picture of a fluid particle pair as a couple of material points rotating around their centre of mass is proposed when the particle separation falls in the inertial range. Since in the centre-of-mass reference frame the particles move only radially, it is possible to derive formulae for relative velocity and relative acceleration, thereby constraining the non-uniqueness problem.

The Lagrangian relative velocity can be written as, see Appendix A,

$$\boldsymbol{u} = u_\parallel \frac{\boldsymbol{r}}{r} + \boldsymbol{\Omega}\times\boldsymbol{r}, \quad (3.1)$$

where

$$\boldsymbol{\Omega} = \frac{1}{r^2}(\boldsymbol{r}\times\boldsymbol{u}). \quad (3.2)$$

In the chosen physical picture, the orientation and the value of the angular velocity vector $\boldsymbol{\Omega}$ (3.2) depend, at all times, on the particle separation and their velocity difference.

In decomposition (3.1), no strain-rate term appears because Lagrangian quantities are considered; the Helmholtz theorem for the decomposition of a vector field as the sum of an irrotational vector and a solenoidal vector holds for space-dependent vectors only, e.g. the Eulerian velocity field (Narasimhan 1993, p. 186). Furthermore, in the determination of the angular velocity $\boldsymbol{\Omega}$, no gauge invariants occur in (3.1)–(3.2), since in this particular case, the rotation axis is perpendicular to the separation line ($\boldsymbol{\Omega} \perp \boldsymbol{r}$); as discussed in Appendix A. The unit mass angular and inertial momenta of each particle with respect to the centre of mass are

https://doi.org/10.1017/S0022112008003820 Published online by Cambridge University Press

$\boldsymbol{M}^{(i)} = (\boldsymbol{r} \times \boldsymbol{u})/4$ and $I^{(i)} = (r/2)^2$, respectively, and the modulus of the angular velocity vector $\Omega = u_\perp / r$.

The Lagrangian relative acceleration is defined as $\boldsymbol{A} = \mathrm{d}\boldsymbol{u}/\mathrm{d}t = \boldsymbol{A}^{(1)} - \boldsymbol{A}^{(2)}$ where $\boldsymbol{A}^{(i)} = \mathrm{d}\boldsymbol{u}^{(i)}/\mathrm{d}t$, and its most general form, when (3.1) holds, is

$$\boldsymbol{A} = \alpha_1 \frac{\boldsymbol{r}}{r} + \alpha_2(\boldsymbol{\Omega} \times \boldsymbol{r}) + \alpha_3(\boldsymbol{r} \times (\boldsymbol{\Omega} \times \boldsymbol{r})). \tag{3.3}$$

Taking the time derivative of (3.1) gives

$$\boldsymbol{A} = \frac{\mathrm{d}\boldsymbol{u}}{\mathrm{d}t} = \left(A_\parallel + \frac{u_\perp^2}{r} \right) \frac{\boldsymbol{r}}{r} + \boldsymbol{\Omega} \times \boldsymbol{u} + \frac{u_\parallel}{r}\boldsymbol{u} - \frac{u_\parallel^2}{r}\frac{\boldsymbol{r}}{r} + \dot{\boldsymbol{\Omega}} \times \boldsymbol{r}, \tag{3.4}$$

where

$$\frac{\mathrm{d}u_\parallel}{\mathrm{d}t} = \frac{\mathrm{d}}{\mathrm{d}t}\frac{u_i r_i}{r} = \frac{(A_i r_i + u_i u_i)r - u_i r_i u_\parallel}{r^2} = A_\parallel + \frac{u_\perp^2}{r}, \quad A_\parallel = \frac{A_i r_i}{r},$$

and $\dot{\boldsymbol{\Omega}} = \mathrm{d}\boldsymbol{\Omega}/\mathrm{d}t$. In the present case, from (3.2) $\dot{\boldsymbol{\Omega}}$ is

$$\dot{\boldsymbol{\Omega}} = \frac{1}{r^2}\left[(\boldsymbol{r} \times \boldsymbol{A}) - 2\frac{u_\parallel}{r}(\boldsymbol{r} \times \boldsymbol{u}) \right].$$

Since $\dot{\boldsymbol{\Omega}}$ substituted into (3.4) gives the identity $\boldsymbol{A} = \boldsymbol{A}$, no constraint can be obtained for the coefficients $\{\alpha_1, \alpha_2, \alpha_3\}$. Using (3.2), formula (3.3) can be rearranged as

$$\boldsymbol{A} = (\alpha_1 - \alpha_2 u_\parallel)\frac{\boldsymbol{r}}{r} + \alpha_2 \boldsymbol{u} + \alpha_3 r^2 \boldsymbol{\Omega}. \tag{3.5}$$

The kinematic formula (3.5) will be related to the drift term of the stochastic model and the coefficients determined from symmetries and properties of the statistical description so that a closure for the non-uniqueness problem is obtained.

Li & Meneveau (2005, 2006) discussed the determination of $\mathrm{d}u_\parallel/\mathrm{d}t$ and $\mathrm{d}u_\perp/\mathrm{d}t$ starting from the linear approximation $u_i(\boldsymbol{x} + \boldsymbol{r}) - u_i(\boldsymbol{x}) = A_{ki} r_k$, where A_{ki}, the velocity gradient tensor $A_{ki} = \partial u_k / \partial x_i$, is considered constant across a fixed length ℓ. In fact, they derived the so called 'advected delta-vee' system of equations for $\mathrm{d}u_\parallel/\mathrm{d}t$ and $\mathrm{d}u_\perp/\mathrm{d}t$, which is useful for the computation of $\boldsymbol{A}$ (3.5). However, in the present paper, the Lagrangian acceleration is determined in the framework of the well-mixed approach. Nevertheless, one of their results will be used in the next section to support the closure derived here.

3.2. *Particle pair rotation and stochastic models*

As pointed out by Kurbanmuradov (1997), in isotropic turbulence, the drift term a_i in Cartesian coordinates has the following general form

$$a_i(u_\parallel, u_\perp, r, t) = \varphi(u_\parallel, u_\perp, r, t)\frac{r_i}{r} + \psi(u_\parallel, u_\perp, r, t)\frac{u_i}{u}, \tag{3.6}$$

where φ and ψ are two unknown scalar functions.

The drift terms in Cartesian and spherical coordinates are related to each other as follows (Risken 1989):

$$\chi_\parallel(u_\parallel, u_\perp, r, t) = a_\parallel + \frac{u_\perp^2}{r} \tag{3.7}$$

$$= \varphi + \psi\frac{u_\parallel}{u} + \frac{u_\perp^2}{r}, \tag{3.8}$$

https://doi.org/10.1017/S0022112008003820 Published online by Cambridge University Press

$$\chi_\perp(u_\parallel, u_\perp, r, t) = \frac{u_i a_i - u_\parallel a_\parallel}{u_\perp} - \frac{u_\parallel u_\perp}{r} + \frac{C_0\varepsilon}{u_\perp} \tag{3.9}$$

$$= \psi\frac{u_\perp}{u} - \frac{u_\parallel u_\perp}{r} + \frac{C_0\varepsilon}{u_\perp}. \tag{3.10}$$

From (3.8) and (3.10), the following expressions for φ and ψ are found:

$$\varphi = \chi_\parallel - \frac{u_\parallel}{u_\perp}\chi_\perp - \frac{u^2}{r} + \frac{u_\parallel}{u_\perp}\frac{C_0\varepsilon}{u_\perp}, \tag{3.11}$$

$$\psi = \frac{u}{u_\perp}\chi_\perp + \frac{u u_\parallel}{r} - \frac{u}{u_\perp}\frac{C_0\varepsilon}{u_\perp}. \tag{3.12}$$

Substitution of (3.11)–(3.12) into (3.6) yields

$$a_i = \chi_\parallel\frac{r_i}{r} + \frac{1}{u_\perp}\left(u_i - u_\parallel\frac{r_i}{r}\right)\left(\chi_\perp - \frac{C_0\varepsilon}{u_\perp}\right) - \frac{u^2}{r^2}r_i + \frac{u_\parallel}{r}u_i, \tag{3.13}$$

and in vector form

$$\boldsymbol{a} = \chi_\parallel\frac{\boldsymbol{r}}{r} + \frac{1}{u_\perp}\left(\boldsymbol{u} - u_\parallel\frac{\boldsymbol{r}}{r}\right)\left(\chi_\perp - \frac{C_0\varepsilon}{u_\perp}\right) + \boldsymbol{\Omega}\times\boldsymbol{u}, \tag{3.14}$$

where the angular velocity $\boldsymbol{\Omega}$ is defined in (3.2). For the noise $\mathrm{d}\boldsymbol{W}$, a representation of the type of (3.6) cannot be given because a Markovian noise is not a function of $\boldsymbol{r}$ or $\boldsymbol{u}$. However, keeping in mind that in the chosen reference frame the motion is only radial with respect to the centre of mass, the noise can be explicitly considered in the longitudinal direction while in the transverse direction it is implicitly taken into account with the dependence of the drift term on the stochastic variable $u_\perp$. Finally, considering also that the noise is not affected by the variables changing (Risken 1989, pp. 57–58, 88–91),

$$\mathrm{d}\boldsymbol{W} = \left(\mathrm{d}\boldsymbol{W}\cdot\frac{\boldsymbol{r}}{r}\right)\frac{\boldsymbol{r}}{r} = \mathrm{d}W_\parallel\frac{\boldsymbol{r}}{r}. \tag{3.15}$$

Hence, considering that

$$\boldsymbol{A}\,\mathrm{d}t = \boldsymbol{a}\,\mathrm{d}t + \sqrt{2C_0\varepsilon}\,\mathrm{d}\boldsymbol{W} \tag{3.16}$$

formally holds (1.1a, b), (3.4), substitution of (3.6) and (3.15) into (3.16) gives

$$\boldsymbol{A}\,\mathrm{d}t = (\varphi\,\mathrm{d}t + \sqrt{2C_0\varepsilon}\,\mathrm{d}W_\parallel)\frac{\boldsymbol{r}}{r} + \psi\frac{\boldsymbol{u}}{u}\,\mathrm{d}t. \tag{3.17}$$

Now, comparing (3.17) and (3.5), the coefficients α_2 and α_3 are determined as $\alpha_2 = \psi/u$ and $\alpha_3 = 0$. Furthermore, the above definition of $A_\parallel$ gives

$$\alpha_1\,\mathrm{d}t = A_\parallel\,\mathrm{d}t = a_\parallel\,\mathrm{d}t + \sqrt{2C_0\varepsilon}\,\mathrm{d}W_\parallel,$$

so that α_1 includes all the effects of the stochastic noise. From comparison of (3.17) and (3.5) the following equation is obtained for φ:

$$\varphi = a_\parallel - \alpha_2 u_\parallel. \tag{3.18}$$

Substitution in (3.18) of φ with (3.11) and of $a_\parallel$ with (3.7) gives

$$\frac{u_\parallel}{u_\perp}\left(\chi_\perp - \frac{C_0\varepsilon}{u_\perp}\right) + \frac{u^2}{r} = \frac{u_\perp^2}{r} + \alpha_2 u_\parallel. \tag{3.19}$$

From (3.15) and arguments above it, the effects of the stochastic noise are only along the $\boldsymbol{r}/r$ direction. Therefore, α_2 appears to be independent of $C_0\varepsilon$ because it is the

https://doi.org/10.1017/S0022112008003820 Published online by Cambridge University Press

coefficient in the $(\boldsymbol{\Omega}\times\boldsymbol{r})/|\boldsymbol{\Omega}\times\boldsymbol{r}|$ direction. This means that $\chi_\perp = C_0\varepsilon/u_\perp + f(u_\parallel, u_\perp, r)$. The system of stochastic equations (2.1*a–c*) gives the evolution in time of $\{u_\parallel, u_\perp, r\}$ with Lagrangian probability density function $p_L(u_\parallel, u_\perp, r; t|r_0)$. This PDF can be composed by the product $p_L(u_\parallel, r; t|u_\perp, r_0)p(u_\perp; t|r_0)$ and from this, in stationary turbulence, it is statistically sound to have $\chi_\perp = \chi_\perp(u_\perp, r)$. From dimensional analysis, $\chi_\perp$ assumes the form

$$\chi_\perp = \frac{C_0\varepsilon}{u_\perp} + k\frac{u_\perp^2}{r},$$

where k is a dimensionless real number which has to be determined. However, for numerical stability, k must be zero. In fact, when $u_\perp$ tends to 0 or $+\infty$, the limits of $\chi_\perp$ with $k \neq 0$ are

$$u_\perp \to 0, \quad \chi_\perp \to +\infty,$$

$$u_\perp \to +\infty, \quad \chi_\perp \to \mathrm{sgn}(k)\,\infty,$$

and with $k = 0$

$$u_\perp \to 0, \quad \chi_\perp \to +\infty,$$

$$u_\perp \to +\infty, \quad \chi_\perp \to 0.$$

Finally, $\chi_\perp$ is given by

$$\chi_\perp = \frac{C_0\varepsilon}{u_\perp}, \tag{3.20}$$

and therefore $\alpha_2 = u_\parallel/r$. With the three coefficients now determined as $\alpha_1 = A_\parallel$, $\alpha_2 = u_\parallel/r$, $\alpha_3 = 0$, (3.3) becomes

$$\boldsymbol{A} = \left(A_\parallel + \frac{u_\perp^2}{r}\right)\frac{\boldsymbol{r}}{r} - \frac{u^2}{r}\frac{\boldsymbol{r}}{r} + \frac{u_\parallel}{r}\boldsymbol{u}, \tag{3.21}$$

and in Cartesian components

$$A_i = \left(A_\parallel + \frac{u_\perp^2}{r}\right)\frac{r_i}{r} - \frac{u^2}{r}\frac{r_i}{r} + \frac{u_\parallel}{r}u_i. \tag{3.22}$$

Furthermore, (3.21) can be rearranged as

$$\boldsymbol{A} = \left(A_\parallel + \frac{u_\perp^2}{r}\right)\frac{\boldsymbol{r}}{r} + \boldsymbol{\Omega}\times\boldsymbol{u}, \tag{3.23}$$

which gives an identity when substituted into (3.4) (see Appendix B). Equation (3.23) is the solution of (3.4) combined with the stochastic model formulae (3.14) and (3.20).

Note that (2.7) in Li & Menevau (2006) is obtained from the above solution (3.23) when substituting $r = \ell$ and changing the sign of α_2. This change of sign means that the growth direction of the $(\boldsymbol{\Omega}\times\boldsymbol{r})/|\boldsymbol{\Omega}\times\boldsymbol{r}|$ axis is inverted (3.3).

The physical picture described above selects a unique model in the well-mixed class, and thereby solves the drift indeterminacy. In fact, applying (1.3) in the new reference frame to the Fokker–Planck equation associated to (2.1*a–c*), and using (3.20), the following equation is obtained (Pagnini 2005):

$$\frac{\partial p_E}{\partial t} + \frac{1}{r^2}\frac{\partial}{\partial r}(r^2 u_\parallel p_E) + \frac{\partial}{\partial u_\parallel}(\chi_\parallel p_E) = C_0\varepsilon\left[\frac{\partial^2 p_E}{\partial u_\parallel^2} + \frac{1}{u_\perp}\frac{\partial}{\partial u_\perp}\left(u_\perp\frac{\partial p_E}{\partial u_\perp}\right)\right], \tag{3.24}$$

https://doi.org/10.1017/S0022112008003820 Published online by Cambridge University Press

with the normalization condition

$$2\pi \int_{-\infty}^{+\infty} \mathrm{d}u_{\parallel} \int_{0}^{+\infty} \mathrm{d}u_{\perp} u_{\perp} p_E(u_{\parallel}, u_{\perp}; t|r) = 1.$$

Integrating (3.24) in $u_{\parallel} \in]-\infty; u_{\parallel}]$, the second drift term $\chi_{\parallel}$ is uniquely determined by

$$\chi_{\parallel} = C_0 \varepsilon \frac{1}{p_E} \frac{\partial p_E}{\partial u_{\parallel}} - \frac{1}{p_E} \Psi(u_{\parallel}, u_{\perp}, r, t), \tag{3.25}$$

where

$$\Psi = \int_{-\infty}^{u_{\parallel}} \left\{ \frac{\partial p_E}{\partial t} + \frac{1}{r^2} \frac{\partial}{\partial r}(r^2 u'_{\parallel} p_E) - \frac{C_0 \varepsilon}{u_{\perp}} \frac{\partial}{\partial u_{\perp}} \left(u_{\perp} \frac{\partial p_E}{\partial u_{\perp}} \right) \right\} \mathrm{d}u'_{\parallel}, \tag{3.26}$$

with the general assumptions

$$\chi_{\parallel} p_E \to 0, \qquad \frac{\partial p_E}{\partial u_{\parallel}} \to 0, \qquad |u_{\parallel}| \to \infty.$$

Equation (3.25) shows the dependence of the longitudinal drift $\chi_{\parallel}$ on $u_{\perp}$, which is different from the longitudinal drift obtained from the quasi-one-dimensional assumption by Kurbanmuradov (1997).

The relative motion between two particles turns out to be described by the stochastic differential equations

$$\mathrm{d}r = u_{\parallel} \, \mathrm{d}t, \quad \mathrm{d}u_{\parallel} = \chi_{\parallel} \, \mathrm{d}t + \sqrt{2C_0 \varepsilon} \, \mathrm{d}W_{\parallel}, \quad \mathrm{d}u_{\perp} = \frac{C_0 \varepsilon}{u_{\perp}} \mathrm{d}t + \sqrt{2C_0 \varepsilon} \, \mathrm{d}W_{\perp}, \tag{3.27a–c}$$

where $\chi_{\parallel}$ is defined in (3.25)–(3.26). From (3.11)–(3.12), the two unknown functions φ and ψ (3.6) are

$$\varphi = \chi_{\parallel} - \frac{u^2}{r}, \quad \psi = \frac{u u_{\parallel}}{r}. \tag{3.28}$$

Mathematically, the multidimensional models are not closed because, for a given Eulerian PDF, there are two unknown functions (φ, ψ) and only one constraint, i.e. the Fokker–Planck equation. In the present approach, there are two unknown functions $(\chi_{\parallel}, \chi_{\perp})$, or equivalently (φ, ψ), and two constraints, i.e. (3.20) and the evolution equation (3.24).

4. Physical aspects of the closure proposed

4.1. *Compatibility with the Navier–Stokes equations*

Since the stochastic models formulation proposed includes the statistical dependence between the longitudinal and the orthogonal components of the velocity difference vector, it is consistent with a fundamental aspect of Navier–Stokes dynamics. On the contrary, the models formulated with the quasi-one-dimensional assumption are inconsistent with this fundamental aspect of Navier–Stokes equations because that assumption is based on the statistical independence of the velocity difference components. The same fundamental inconsistency with Navier–Stokes equations occurs for Gaussian models formulated in Cartesian coordinates (Thomson 1990; Borgas & Sawford 1994) because they are based on the covariance matrix of velocity difference that reduces to a diagonal matrix (i.e. statistical independence of velocity difference components) when the present reference frame is adopted.

In stationary isotropic turbulence, one of the few exact results of the Navier–Stokes equations is the so-called 4/5 law that affirms (see Monin & Yaglom 1975; Frisch

https://doi.org/10.1017/S0022112008003820 Published online by Cambridge University Press

1996)

$$\langle u_\parallel^3 \rangle = -\tfrac{4}{5}\varepsilon r. \tag{4.1}$$

The two perpendicular components $u'_\perp$ and $u''_\perp$ are such that $u_\perp^2 = u_\perp'^2 + u_\perp''^2$ and $\langle u_\perp^2 \rangle = 2\langle u_\perp'^2 \rangle = 2\langle u_\perp''^2 \rangle$, then for a solenoidal isotropic field (see Monin & Yaglom 1975, p. 107, Frisch 1996)

$$\begin{aligned} \tfrac{1}{2}\langle u_\parallel u_\perp^2 \rangle = \langle u_\parallel u_\perp'^2 \rangle &= \tfrac{1}{6}\left[\langle u_\parallel^3 \rangle + r\frac{\partial \langle u_\parallel^3 \rangle}{\partial r} \right] \\ &= -\tfrac{4}{15}\varepsilon r, \end{aligned} \tag{4.2}$$

and for each Cartesian component

$$\langle u_i u_j u_k \rangle = -\tfrac{4}{15}\varepsilon(r_i\delta_{jk} + r_j\delta_{ik} + r_k\delta_{ij}). \tag{4.3}$$

The exact result (4.2) shows that the components of the velocity difference are not statistically independent, as a consequence the Eulerian PDF cannot be factorized. This result is of fundamental importance in turbulent dynamics. In fact, the moment of the third order represents the energy transport between the motions of various scales, and this is a major feature of turbulent flow (Novikov 1989). This strong physical constraint arises naturally in the formulation derived here. In fact, in the stationary case ($\partial p_E/\partial t = 0$) integrating (3.24) in $u_\parallel \in]-\infty;+\infty[$ with weight 2π gives

$$\frac{1}{r^2}\frac{\partial}{\partial r}(r^2\langle u_\parallel | u_\perp \rangle p_\perp) = \frac{C_0\varepsilon}{u_\perp}\frac{\partial}{\partial u_\perp}\left(u_\perp \frac{\partial p_\perp}{\partial u_\perp} \right), \tag{4.4}$$

where $p_\perp$ is the marginal PDF of $u_\perp$ ($p_\perp = p_E(u_\perp) = 2\pi \int p_E \, \mathrm{d}u_\parallel$) and $\langle u_\parallel | u_\perp \rangle$ is the conditional mean defined as

$$\langle u_\parallel | u_\perp \rangle = 2\pi \int_{-\infty}^{\infty} u_\parallel p_E(u_\parallel | u_\perp) \, \mathrm{d}u_\parallel, \quad p_E(u_\parallel | u_\perp) = \frac{p_E(u_\parallel, u_\perp)}{p_E(u_\perp)}.$$

Then, if the Eulerian PDF can be factorized, the equalities $\langle u_\parallel | u_\perp \rangle = \langle u_\parallel \rangle = 0$ hold and (4.4) becomes

$$u_\perp^2 \frac{\partial^2 p_\perp}{\partial u_\perp^2} + u_\perp \frac{\partial p_\perp}{\partial u_\perp} = 0, \tag{4.5}$$

after multiplication by $u_\perp^2$. However, it is well known that for a function $h(\xi)$, $\xi \in R^+$, the following Mellin transform rule holds (Sneddon 1972, p. 268)

$$\xi^2 \frac{\partial^2 h}{\partial \xi^2} + \xi \frac{\partial h}{\partial \xi} \overset{\mathscr{M}}{\longleftrightarrow} s^2 h^*(s), \tag{4.6}$$

hence (4.5) is solved, in the s space, by

$$s^2 p_\perp^*(s) = 0. \tag{4.7}$$

From (4.7), it is clear that there is no non-trivial solution to (4.5). This proves that in this closure scheme, the choice of a factorizable Eulerian PDF of the velocity difference is not permitted in the inertial range. However, in § 4.4, it will be shown that in the small-length-scale limit and spatial decorrelated velocity field, a Gaussian Eulerian PDF is recovered.

This result makes the approach derived here strongly different from the other ones. In fact, in the quasi-one-dimensional approach (Kurbanmuradov 1997), the Eulerian statistics generated by the model are consistent with a factorizable Eulerian PDF.

https://doi.org/10.1017/S0022112008003820 Published online by Cambridge University Press

From the stochastic differential equations (2.1*a–c*), with the quasi-one-dimensional assumption $\chi_\parallel = \chi_\parallel(u_\parallel, r, t)$, it follows that the Lagrangian statistics of $u_\parallel$ are independent of $u_\perp$ and then in terms of PDF

$$p_L(u_\parallel, u_\perp, r; t|r_0) = p_L(u_\parallel, r; t|r_0)p(u_\perp),$$

where $p(u_\perp)$ is an undetermined function and depends exclusively on $u_\perp$, as a consequence of the assumption that $\{r, u_\parallel\}$ are independent of $u_\perp$. From (1.3), the Eulerian PDF is

$$\begin{aligned} p_E(u_\parallel, u_\perp; t|r) &= \int p_L(u_\parallel, u_\perp, r; t|r_0)\frac{r_0^2}{r^2}\,\mathrm{d}r_0 \\ &= p(u_\perp)\int p_L(u_\parallel, r; t|r_0)\frac{r_0^2}{r^2}\,\mathrm{d}r_0 \\ &= p(u_\perp)p_E(u_\parallel; t|r). \end{aligned}$$

Now, formula $p_E(u_\parallel, u_\perp; t|r) = p_E(u_\perp; t|r, u_\parallel)p_E(u_\parallel; t|r)$ implies $p_E(u_\perp; t|r, u_\parallel) = p(u_\perp) = p_E(u_\perp)$. As pointed out in (4.2), this statistical independence is in contrast with the Navier–Stokes equations. Moreover, the fact that $u_\parallel$ is statistically independent of $u_\perp$, as follows directly from the quasi-one-dimensional assumption, is in contrast with the Navier–Stokes equations also in the Lagrangian frame. Figure 1(*a*) shows the plot of $\langle u_\parallel|u_\perp\rangle/\langle u_\parallel^2\rangle^{1/2}$ *vs* $\cdot\, u_\perp/\langle u_\perp^2\rangle^{1/2}$ and figure 1(*b*) $\langle u_\perp|u_\parallel\rangle/\langle u_\perp^2\rangle^{1/2}$ *vs* $\cdot\, u_\parallel/\langle u_\parallel^2\rangle^{1/2}$ as computed from the Lagrangian data of the DNS (Biferale *et al.* 2005). From these figures, the statistical dependence between $u_\parallel$ and $u_\perp$ is evident. Both graphs have significant statistical noise for large abscissa values, as the number of particle pairs having large fluctuation is small. However, a strong correlation between $u_\parallel$ and $u_\perp$ is evident when the figure 1(*a*) abscissa is less than 2 and the figure 1(*b*) abscissa ranges between −2 and 2. Furthermore, in these cases of strong correlation, a linear relation occurs in both figures 1(*a*) and 1(*b*). This strong correlation occurs for decreasing abscissa values when the time elapsed from the initial condition is increasing. This can be understood by the fact that the whole process decorrelates when the elapsed time increases.

Equations (4.4)–(4.7) show that the approach proposed here is not compatible with the quasi-one-dimensional assumption. Moreover, the strong characteristic of the Navier–Stokes dynamics of generating statistical dependence between the longitudinal and the orthogonal components of the velocity increments cannot be disregarded in the present formulation. The explicit rotation term causes this statistical dependence and the following non-factorability of the Eulerian PDF.

4.2. *Mean rotation analysis*

The Lagrangian stochastic model formulation proposed is based on a non-zero angular velocity $\boldsymbol{\Omega}$ (3.2), which causes the statistical dependence between the longitudinal and orthogonal components of the velocity difference. The effects of this non-zero angular velocity on the mean rotation are now discussed.

Sawford (1999) introduced the following measure of the rotation

$$\mathrm{d}\boldsymbol{s} = \boldsymbol{u} \times \mathrm{d}\boldsymbol{u}, \tag{4.8}$$

$\mathrm{d}\boldsymbol{u}$ being known from the stochastic model (1.1*a*, *b*). Equation (4.8) can be averaged in the Eulerian way (Sawford 1999) to study the mean rotation effects as follows

$$\langle \mathrm{d}\boldsymbol{s}\rangle = \langle \boldsymbol{u} \times \boldsymbol{a}\rangle\,\mathrm{d}t, \tag{4.9}$$

where the fact that the Wiener process has zero mean is used.

https://doi.org/10.1017/S0022112008003820 Published online by Cambridge University Press

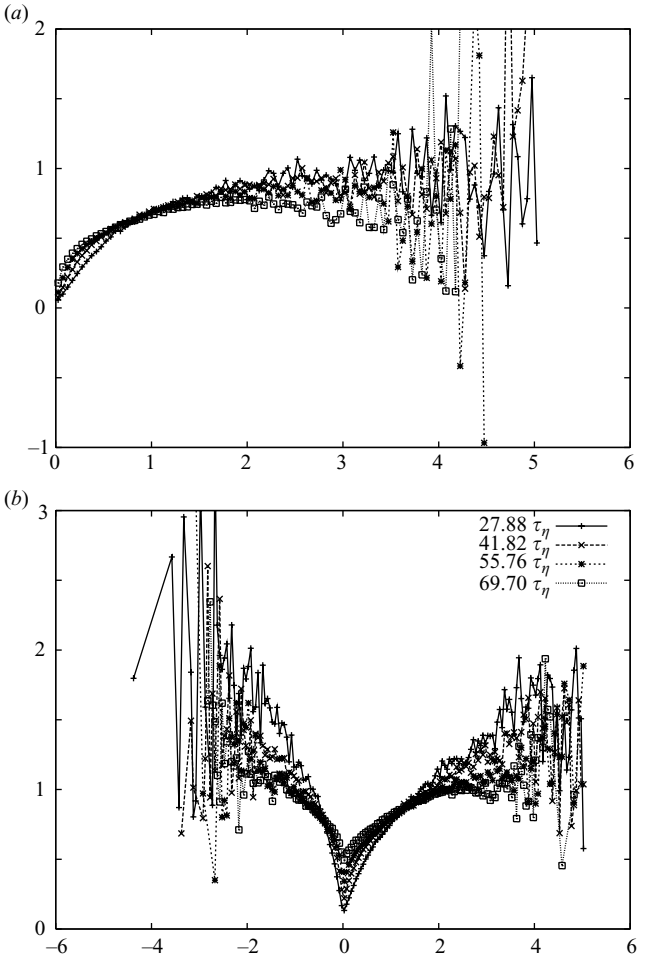


FIGURE 1. The scaled conditional mean (*a*) $\langle u_\parallel | u_\perp \rangle / \langle u_\parallel^2 \rangle^{1/2}$ *vs.* $u_\perp / \langle u_\perp^2 \rangle^{1/2}$ and (*b*) $\langle u_\perp | u_\parallel \rangle / \langle u_\perp^2 \rangle^{1/2}$ *vs.* $u_\parallel / \langle u_\parallel^2 \rangle^{1/2}$ computed from the DNS data with $R_\lambda = 284$ (Biferale *et al.* 2005) at times $t = 27.88\tau_\eta, 41.82\tau_\eta, 55.76\tau_\eta, 69.70\tau_\eta$. The plots show the statistical correlation between the Lagrangian $u_\parallel$ and $u_\perp$; in particular, this correlation is strong when abscissa in (*a*) is less than 2 and the abscissa in (*b*) ranges between -2 and 2.

The drift coefficient in (3.14), after imposing (3.20), is composed by two terms and (4.9) becomes

$$\langle \mathrm{d}\boldsymbol{s} \rangle = -r \langle \chi_\parallel \boldsymbol{\Omega} \rangle \, \mathrm{d}t + \langle \boldsymbol{u} \times \boldsymbol{R} \rangle \, \mathrm{d}t,$$

with $\boldsymbol{R} = \boldsymbol{\Omega} \times \boldsymbol{u}$. It is of interest to study the mean rotation effects introduced by $\boldsymbol{R}$, because the value of $\langle \chi_\parallel \boldsymbol{\Omega} \rangle$ depends on the choice of the Eulerian PDF p_E (3.25)–(3.26). Let $\langle \mathrm{d}\boldsymbol{s}^R \rangle$ be

$$\langle \mathrm{d}\boldsymbol{s}^R \rangle = \langle \boldsymbol{u} \times \boldsymbol{R} \rangle \, \mathrm{d}t = \langle \boldsymbol{u} \times (\boldsymbol{\Omega} \times \boldsymbol{u}) \rangle \, \mathrm{d}t.$$

When using the following vector identity $\boldsymbol{u} \times (\boldsymbol{\Omega} \times \boldsymbol{u}) = \boldsymbol{\Omega}(\boldsymbol{u} \cdot \boldsymbol{u}) - \boldsymbol{u}(\boldsymbol{u} \cdot \boldsymbol{\Omega})$, $\langle \mathrm{d}\boldsymbol{s}^R \rangle$ becomes

$$\langle \mathrm{d}\boldsymbol{s}^R \rangle = \langle \boldsymbol{\Omega}(\boldsymbol{u} \cdot \boldsymbol{u}) \rangle \, \mathrm{d}t - \langle \boldsymbol{u}(\boldsymbol{u} \cdot \boldsymbol{\Omega}) \rangle \, \mathrm{d}t,$$

https://doi.org/10.1017/S0022112008003820 Published online by Cambridge University Press

and for the Cartesian components this yields

$$\left\langle \mathrm{d}s_i^R \right\rangle = \langle \boldsymbol{\Omega}_i(\boldsymbol{u}\cdot\boldsymbol{u})\rangle\,\mathrm{d}t - \langle u_i(\boldsymbol{u}\cdot\boldsymbol{\Omega})\rangle\,\mathrm{d}t. \tag{4.10}$$

Now, including (3.2) in (4.10), we obtain

$$\left\langle \mathrm{d}s_i^R \right\rangle = \frac{1}{r^2}[\langle(\varepsilon_{ijk}r_j u_k)u^2\rangle - \langle u_i u_i(\varepsilon_{ijk}r_j u_k)\rangle + \langle u_i u_j(\varepsilon_{jki}r_k u_i)\rangle + \langle u_i u_k(\varepsilon_{kij}r_i u_j)\rangle]\,\mathrm{d}t,$$

and finally

$$\left\langle \mathrm{d}s_i^R \right\rangle = 0.$$

It is therefore possible to conclude that the effect of the angular velocity term (3.2) on the mean rotation is zero. This is consistent with the isotropy of the flow.

4.3. *Compatibility with the vorticity field*

The approach derived here is based on the decomposition of the two-point velocity vector (3.1). This decomposition is physically based on the idea that the two-particle dispersion process has a non-zero angular velocity $\boldsymbol{\Omega}$ (3.2) that, as it will be shown in this section, makes the present closure consistent with a non-zero vorticity field. As pointed out in (Monin & Yaglom 1975, p. 374) the statistical characteristics of the vorticity field are related to the two-point Eulerian statistics. For the relationship between relative dispersion and the two-point Eulerian theory, the consistency of a two-particle Lagrangian model with the vorticity field is an important aspect.

Longitudinal and orthogonal correlation functions of the vorticity field can be expressed in terms of the longitudinal Eulerian second-order velocity structure function $S_E = \langle[(\boldsymbol{U}(\boldsymbol{x}) - \boldsymbol{U}(\boldsymbol{x}+\boldsymbol{r}))\cdot\boldsymbol{r}/r]^2\rangle = C_K(\varepsilon r)^{2/3}$, where $\boldsymbol{U}(\boldsymbol{x})$ is the velocity in point $\boldsymbol{x}$ and C_K the Kolmogorov constant. As a consequence, the vorticity field is non-zero. This observation makes a non-zero angular velocity $\boldsymbol{\Omega}$ necessary in the decomposition (3.1)–(3.2). In fact, the vorticity field is defined in a single point $\boldsymbol{x}$ as $\boldsymbol{\omega}(\boldsymbol{x}) = \nabla_{\boldsymbol{x}} \times \boldsymbol{U}(\boldsymbol{x})$, and then being (see Hill 2002)

$$\frac{\partial}{\partial r_i} = \frac{1}{2}\left(\frac{\partial}{\partial x_i} - \frac{\partial}{\partial x_i'}\right), \quad \boldsymbol{r} = \boldsymbol{x} - \boldsymbol{x}',$$

with $\boldsymbol{u}(\boldsymbol{r}) = \boldsymbol{U}(\boldsymbol{x}) - \boldsymbol{U}(\boldsymbol{x}+\boldsymbol{r})$ it follows that

$$\begin{aligned}\boldsymbol{\omega}(\boldsymbol{x}) + \boldsymbol{\omega}(\boldsymbol{x}') &= 2\,[\nabla_{\boldsymbol{r}} \times \boldsymbol{u}(\boldsymbol{r})] \\ &= 2\left[\nabla_{\boldsymbol{r}} \times \left(u_{\parallel}\frac{\boldsymbol{r}}{r}\right) + \nabla_{\boldsymbol{r}} \times (\boldsymbol{\Omega} \times \boldsymbol{r})\right] \\ &= 2\,[-\boldsymbol{\Omega} + \nabla_{\boldsymbol{r}} \times (\boldsymbol{\Omega} \times \boldsymbol{r})]\,.\end{aligned}$$

For the arbitrariness of $\boldsymbol{x}$ and $\boldsymbol{x}'$, if $\boldsymbol{\Omega} = 0$, the latter equation requires the unsatisfactory result $\boldsymbol{\omega}(\boldsymbol{x}) = \boldsymbol{\omega}(\boldsymbol{x}') = 0$. As a consequence, decomposition (3.1)–(3.2), which is a fundamental part of the approach derived here, guarantees a correct non-null vorticity field. On the other hand, this means that any model formulation without particle pair rotation (i.e. with a zero angular velocity $\boldsymbol{\Omega}$) is not in agreement with the non-zero vorticity field.

4.4. *The small-length-scale limit and the large-fluctuation regime*

The strong connection between turbulent relative dispersion and two-point Eulerian theory suggests, as important, the issue of the small-length-scale limit. Besides this, also the large-fluctuation regime ($u^2 \gg \langle u^2\rangle$) has an important role in turbulent dispersion. This last was studied for the first time by Novikov (1992) with particular

https://doi.org/10.1017/S0022112008003820 Published online by Cambridge University Press

attention to the form of the Eulerian PDF. The large-fluctuation regime 'physically corresponds to motions with large local shear of velocity or to local jetlike motions ("streaks"), when one of the fluid particles is inside the jet and another is outside. In this case, the inertial term, subject to the incompressibility condition, should dominate' (Novikov 1992). These two asymptotic regimes correspond to the same mathematical constraint. A similar study can be found in Pedrizzetti & Novikov (1994).

In stationary, homogeneous and incompressible flow, the continuity equation for the Eulerian PDF, or the transport equation, has the form (Pope 1985; Novikov 1992; Heppe 1998)

$$u_i \frac{\partial p_E}{\partial r_i} + \frac{\partial}{\partial u_i}\left[\left\langle \frac{\mathrm{D}U_i}{\mathrm{D}t} | \boldsymbol{u}, \boldsymbol{r} \right\rangle p_E\right] = 0, \tag{4.11}$$

where $\mathrm{D}U_i/\mathrm{D}t$ represents the two-point Navier–Stokes equation and $\langle \cdot | \boldsymbol{u}, \boldsymbol{r}\rangle$ the conditional mean. Equation (4.11) can be compared with the evolution equation obtained applying (1.3) to the Fokker–Planck equation for the Lagrangian PDF (1.2), and this yields $a_i = \langle \mathrm{D}U_i/\mathrm{D}t | \boldsymbol{u}, \boldsymbol{r}\rangle + C_0\varepsilon \partial \log p_E/\partial u_i$. In the case considered, from (3.7) and (3.9) the transport equation (4.11) turns out to be

$$\begin{aligned}\frac{1}{r^2}\frac{\partial}{\partial r}(r^2 u_\parallel p_E) + \frac{\partial}{\partial u_\parallel}\left[\left\langle \frac{\mathrm{D}\boldsymbol{U}}{\mathrm{D}t}\cdot\frac{\boldsymbol{r}}{r} + \frac{U_\perp^2}{r} | \boldsymbol{u}, \boldsymbol{r}\right\rangle p_E\right] \\ + \frac{\partial}{\partial u_\perp}\left[\left\langle \frac{1}{U_\perp}\left(U_i\frac{\mathrm{D}U_i}{\mathrm{D}t} - U_\parallel \frac{\mathrm{D}\boldsymbol{U}}{\mathrm{D}t}\cdot\frac{\boldsymbol{r}}{r}\right) - \frac{U_\perp U_\parallel}{r} | \boldsymbol{u}, \boldsymbol{r}\right\rangle p_E\right] = 0.\end{aligned}$$

Using (3.22), this becomes

$$\frac{1}{r^2}\frac{\partial}{\partial r}(r^2 u_\parallel p_E) + \frac{\partial}{\partial u_\parallel}\left[\left\langle \frac{\mathrm{D}\boldsymbol{U}}{\mathrm{D}t}\cdot\frac{\boldsymbol{r}}{r} + \frac{U_\perp^2}{r} | \boldsymbol{u}, \boldsymbol{r}\right\rangle p_E\right] = 0, \tag{4.12}$$

where both $\langle (\mathrm{D}\boldsymbol{U}/\mathrm{D}t)\cdot(\boldsymbol{r}/r) + (U_\perp^2/r) | \boldsymbol{u}, \boldsymbol{r}\rangle$ and p_E are functions of $\{u_\parallel, u_\perp, r\}$ and from (3.24) it follows that

$$\begin{aligned}\left\langle \frac{\mathrm{D}U_\parallel}{\mathrm{D}t} | \boldsymbol{u}, \boldsymbol{r}\right\rangle &= \left\langle \frac{\mathrm{D}\boldsymbol{U}}{\mathrm{D}t}\cdot\frac{\boldsymbol{r}}{r} + \frac{U_\perp^2}{r} | \boldsymbol{u}, \boldsymbol{r}\right\rangle \\ &= \left\langle \frac{\mathrm{D}\boldsymbol{U}}{\mathrm{D}t}\cdot\frac{\boldsymbol{r}}{r} | \boldsymbol{u}, \boldsymbol{r}\right\rangle + \frac{u_\perp^2}{r} \\ &= \chi_\parallel(u_\parallel, u_\perp, r) - \frac{C_0\varepsilon}{p_E}\left[\frac{\partial p_E}{\partial u_\parallel} + \frac{1}{u_\perp}\frac{\partial}{\partial u_\perp}\left(u_\perp \frac{\partial}{\partial u_\perp}\int_{-\infty}^{u_\parallel} p_E \mathrm{d}u'_\parallel\right)\right].\end{aligned} \tag{4.13}$$

It is important to remark that, although (4.12) is a partial differential equation in $(r, u_\parallel)$, the Eulerian PDF p_E and the term $\langle (\mathrm{D}\boldsymbol{U}/\mathrm{D}t)\cdot(\boldsymbol{r}/r) + U_\perp^2/r | \boldsymbol{u}, \boldsymbol{r}\rangle$ are functions of $(r, u_\parallel, u_\perp)$. This is consistent with the fact that in the isotropic case the statistics of $u_\perp$ are related to those of $u_\parallel$.

Since in the small-length-scale limit the process is in equilibrium, the velocity is completely uncorrelated and the two-point Eulerian statistics turn out to be independent of r, i.e. $p_E = p_E(\boldsymbol{u})$. Indeed, in the large-fluctuation regime, the inertial term dominates (Novikov 1992) and the spatial derivative is neglected even if the two-point Eulerian statistics are still dependent on the particle separation, i.e. $p_E = p_E(\boldsymbol{u}|r)$. Then, in both asymptotic regimes, studying (4.11) is equivalent to analysing the constraint

$$\frac{\partial}{\partial r_i}(u_i p_E) = 0, \tag{4.14}$$

https://doi.org/10.1017/S0022112008003820 Published online by Cambridge University Press

but in the two previous strongly different physical conditions. In the spherical frame, constraint (4.14) is given by

$$u_\parallel \frac{\partial p_E}{\partial r} + \frac{u_\perp^2}{r}\frac{\partial p_E}{\partial u_\parallel} - \frac{u_\parallel u_\perp}{r}\frac{\partial p_E}{\partial u_\perp} = 0. \tag{4.15}$$

In the small-length-scale limit ($\partial p_E/\partial r = 0$), condition (4.15) becomes

$$\frac{1}{u_\parallel}\frac{\partial p_E}{\partial u_\parallel} = \frac{1}{u_\perp}\frac{\partial p_E}{\partial u_\perp}, \tag{4.16}$$

and the Eulerian PDF is Gaussian

$$p_E(u_\parallel, u_\perp) = \frac{1}{(2\pi)^{3/2}\sigma^3}\exp\left\{-\frac{u_\parallel^2 + u_\perp^2}{2\sigma^2}\right\}, \tag{4.17}$$

with $\langle u_\parallel^2\rangle = \sigma^2$ and $\langle u_\perp^2\rangle = 2\langle u_\parallel^2\rangle = 2\sigma^2$. The stochastic process (1.1a, b) turns out to be an Ornstein–Uhlenbeck process where $a_i = -u_i/\tau_L$, and τ_L is an inertial range Lagrangian time scale defined by Tennekes (1982) as

$$\tau_L = \frac{\sigma^2}{C_0\varepsilon} = \frac{2\sigma_{1_p}^2}{C_0\varepsilon}, \tag{4.18}$$

where $\sigma_{1_p}^2$ is the one-point velocity variance.

In the large-fluctuation regime, using the K41 scaling, the Eulerian PDF which is the solution to (4.15) is a function of the following type (Novikov 1992):

$$p_E(u_\parallel, u_\perp; r) = F(u, u_\perp r) = (\varepsilon r u_\perp)^{-3/4} F_0\left[\frac{u_\parallel^2 + u_\perp^2}{(\varepsilon r u_\perp)^{1/2}}\right]. \tag{4.19}$$

This is an unexpected form of the joint probability and it is strongly non-Gaussian. The odd moments of $u_\parallel$ vanish in this regime because p_E is an even function of $u_\parallel$ (4.19).

If condition (4.15) is derived for the approach proposed here, the following identity is obtained:

$$\frac{1}{r^2}\frac{\partial}{\partial r}(u_\parallel r^2 p_E) + \frac{u_\perp^2}{r}\frac{\partial p_E}{\partial u_\parallel} - \frac{1}{u_\perp}\frac{\partial}{\partial u_\perp}[(a_i u_i - a_\parallel u_\parallel)p_E] = 0. \tag{4.20}$$

It is possible to verify that (4.20) reduces to (4.15), when constraint (3.20) is applied. The correct behaviour of the approach proposed here for these two asymptotic limits is another interesting feature besides the non-factorizability of the Eulerian PDF, as discussed in §4.1. In fact, while the small-length-scale limit is assured for Gaussian models (Thomson 1990; Borgas & Sawford 1994), the large-fluctuation regime is not, because the Eulerian PDF should be non-Gaussian. The quasi-one-dimensional assumption is not compatible with the small-length-scale limit; in fact, when $a_i = -u_i/\tau_L$, formula (3.7) gives $\chi_\parallel = -u_\parallel/\tau_L + u_\perp^2/r$. Moreover, the large-fluctuation regime requires a non-factorizable Eulerian PDF and this cannot be reproduced by the quasi-one-dimensional assumption.

5. Formulation of a Markov model

5.1. *A quadratic model*

To complete the previous study, a simple illustrative Markov model is developed in the approach outlined above and the results are compared with the DNS data by Biferale

https://doi.org/10.1017/S0022112008003820 Published online by Cambridge University Press

R_λ	u_{rms}	ε	ν	η	L	T_E	τ_η	T	δx	N^3	N_p
284	1.7	0.81	0.00088	0.005	3.14	1.8	0.033	4.4	0.006	1024^3	$1.92 \cdot 10^6$

TABLE 1. DNS parameters: microscale Reynolds numbers R_λ, velocity root mean square u_{rms}, mean turbulent kinetic energy dissipation ε, viscosity ν, Kolmogorov space scale $\eta = (\nu^3/\varepsilon)^{1/4}$, integral space scale L, eddy turnover time $T_E = L/u_{rms}$, Kolmogorov time scale $\tau_\eta = (\nu/\varepsilon)^{1/2}$, total time T, grid step δx, resolution N^3, number of particles N_p.

Reference	R_λ
Sawford *et al.* (2005)	~ 38
Borgas & Yeung (2004)	$\sim 90, 230$
Kurbanmuradov *et al.* (2001)	~ 240
Sawford & Yeung (2000)	~ 148
Heppe (1998)	$\sim 90, 140$
Borgas & Yeung (1998)	$\sim 38, 90, 140, 180, 240$

TABLE 2. The value of the Reynolds number R_λ in a number of recent comparisons between Markov models and DNS.

et al. (2005) on a cubic lattice 1024^3 with Reynolds number $R_\lambda \sim 284$ (see table 1). Following the well-mixed approach, a stochastic model can be formulated when an Eulerian PDF (which includes the flow statistics) is given. Although in stochastic models the intermittency and viscous range effects can be accounted for, here they are neglected to avoid free parameters and parameterization effects. This choice permits a completely parameter-free model for the inertial range. As a consequence, when particle separation falls inside the viscous range, the failure of the model is expected. Comparing DNS data of a moderate R_λ with a model that takes into account the inertial range only, does not seem fully appropriate. However, the DNS dataset used is among those with highest Reynolds numbers available in literature. Recent comparisons between Markov models and DNS have lower value of R_λ than the one considered here (see table 2).

In the K41 case, for dimensional reasons, the Eulerian PDF can be written as

$$p_E = f(u_\parallel, u_\perp, r, \lambda, \varepsilon) = \begin{cases} (\varepsilon r)^{-1} f_0\left(\dfrac{u_\parallel}{(\varepsilon r)^{1/3}}, \dfrac{u_\perp}{(\varepsilon r)^{1/3}}, \dfrac{\lambda}{r}\right), & r < \lambda, \\ (4.17), & r > \lambda, \end{cases} \tag{5.1}$$

where λ is a length scale, and the Eulerian statistics are computed by

$$m_{k,n} = \langle u_\parallel^k u_\perp^n \rangle = 2\pi \int_{-\infty}^{+\infty} \mathrm{d}u_\parallel \int_0^{+\infty} \mathrm{d}u_\perp u_\perp u_\parallel^k u_\perp^n p_E(u_\parallel, u_\perp; t|r), \tag{5.2}$$

so that

$$m_{k,n} = \begin{cases} C_{k,n}(\varepsilon r)^{(k+n)/3}, & r < \lambda, \\ \text{Gauss}, & r > \lambda. \end{cases} \tag{5.3}$$

In particular, it is $m_{0,0} = 1$ for the normalization condition and in the inertial range

$$\begin{gathered} m_{1,0} = 0, \quad m_{2,0} = C_K(\varepsilon r)^{2/3}, \quad m_{3,0} = -\tfrac{4}{5}\varepsilon r, \\ m_{1,1} = 0, \quad m_{1,2} = -\tfrac{8}{15}\varepsilon r, \quad m_{0,2} = \tfrac{8}{3} m_{2,0}. \end{gathered} \tag{5.4}$$

https://doi.org/10.1017/S0022112008003820 Published online by Cambridge University Press

The stochastic model is uniquely defined adopting the constraint (3.20) and substituting (5.1) in (3.25)–(3.26). However, with (3.20), the drift term a_i (3.6) becomes

$$a_i = \varphi \frac{r_i}{r} + \frac{u_\parallel u_i}{r}. \tag{5.5}$$

To avoid mathematical difficulties, the choice of p_E can be reduced to the choice of φ. Making this choice, particular attention has to be paid to the longitudinal component, because it is strictly related to the particle separation r, i.e. $\mathrm{d}r/\mathrm{d}t = u_\parallel$. Here, the following simple choice of φ is studied

$$\varphi = -\frac{u_\parallel}{\tau(r)} + \gamma \frac{u_\parallel^2}{r} + \frac{1}{2}\frac{u_\perp^2}{r} + \rho \frac{u_\parallel u_\perp}{r}, \tag{5.6}$$

where $\{\gamma, \rho\}$ are the model parameters, which will be determined by imposing Eulerian statistics. The relaxation time, denoted by $\tau(r)$, depends on the particle separation and is defined as

$$\tau(r) = \frac{\langle u_\parallel^2 \rangle}{C_0 \varepsilon}. \tag{5.7}$$

In the limit $r \gg \lambda$, (5.7) reduces to $\tau = \tau_L = 2\sigma_{1p}^2/(C_0\varepsilon)$, i.e. the inertial-range Lagrangian time scale (4.18). Factor $1/2$ in front of $u_\perp^2$ in (5.6) is the average of the two perpendicular components being $u_\perp^2 = u_\perp'^2 + u_\perp''^2$ and ρ turns out to be a coupling parameter of the longitudinal and the orthogonal components. In this case,

$$a_i = \left(-\frac{u_\parallel}{\tau(r)} + \gamma \frac{u_\parallel^2}{r} + \frac{1}{2}\frac{u_\perp^2}{r} + \rho \frac{u_\parallel u_\perp}{r} \right) \frac{r_i}{r} + \frac{u_\parallel u_i}{r}, \tag{5.8}$$

and from (3.7) it follows that

$$\chi_\parallel = -\frac{u_\parallel}{\tau(r)} + (\gamma + 1)\frac{u_\parallel^2}{r} + \frac{3}{2}\frac{u_\perp^2}{r} + \rho \frac{u_\parallel u_\perp}{r}. \tag{5.9}$$

5.2. *Model parameter determination by incompressibility and Eulerian statistics*

5.2.1. *Determination of γ*

To ensure the incompressibility in stochastic model, the following condition must hold (Novikov 1989, 1992; Pedrizzetti & Novikov 1994; Pedrizzetti 1999):

$$\langle a_i \rangle = 0, \tag{5.10}$$

so using formula (Monin & Yaglom 1975, p. 102)

$$\langle u_i u_j \rangle = \left[\langle u_\parallel^2 \rangle - \tfrac{1}{2}\langle u_\perp^2 \rangle \right] \frac{r_i r_j}{r^2} + \tfrac{1}{2}\langle u_\perp^2 \rangle \delta_{ij}, \tag{5.11}$$

and the inertial range moments $\{m_{1,0}, m_{2,0}, m_{0,2}, m_{1,1}\}$ in (5.4), it follows that

$$\gamma = -\tfrac{4}{3} - 1 = -\tfrac{7}{3}. \tag{5.12}$$

5.2.2. *Determination of ρ*

The parameter ρ is determined by imposing the consistency with some other Eulerian statistical moments, as in the moments approximation approach. In this case, Eulerian statistics have to be consistent with K41 theory. Multiplying (3.24) by $u_\parallel^k u_\perp^n$, with $k \neq 0$, and integrating with respect to $2\pi u_\perp \, \mathrm{d}u_\parallel \, \mathrm{d}u_\perp$, see (5.2),

https://doi.org/10.1017/S0022112008003820 Published online by Cambridge University Press

yields

$$\frac{2}{r}m_{k+1,n} + \frac{\partial}{\partial r}m_{k+1,n} + \frac{k}{\tau}m_{k,n} + \frac{4}{3}\frac{k}{r}m_{k+1,n} - \frac{3}{2}\frac{k}{r}m_{k-1,n+2} - \rho\frac{k}{r}m_{k,n+1} = C_0\varepsilon\{k(k-1)m_{k-2,n} + n^2 m_{k,n-2}\}. \tag{5.13}$$

Equation (5.13) gives a relationship among all the Eulerian statistics of the Markov model (5.9). The moment exponent k must be $k \neq 0$, otherwise the equation for moments (5.13) turns out to be independent of the drift term $\chi_\parallel$, as follows from (3.24), and it becomes the same equation for moments of a pure diffusive model in the longitudinal velocity space ($\chi_\parallel = 0$). In this case, when $\boldsymbol{\Omega} \neq 0$, the process is compressible because $\langle a_i \rangle = -\langle u_\perp^2 \rangle r_i / r^2 \neq 0$, when $\boldsymbol{\Omega} = 0$ (the equilibrium regime), unphysical results are obtained because $a_i = 0$ (Pedrizzetti & Novikov 1994). The consistency with the K41 Eulerian statistics can be imposed by selecting certain values for k and n. In particular, with $\{k = 1,\ n = 0\}$ condition (5.12) is recovered and requires consistency with: $m_{1,0}$, $m_{2,0}$, $m_{0,2}$, $m_{1,1}$. Moreover, with $\{k = 3,\ n = 0\}$, the consistency with Eulerian statistics is up to the fourth order: $m_{3,0}$, $m_{4,0}$, $m_{2,2}$, $m_{3,1}$. It is worth noting that, in spite of this simple case study, model (5.9) is in agreement with more Eulerian statistics than previous models found in literature (see Pedrizzetti & Novikov 1994; Heppe 1998; Borgas & Yeung 2004). Moreover, from the consistency with $m_{3,0}$ and incompressibility, the consistency with $m_{1,2}$ (4.2) follows. Indeed, knowledge of $m_{4,0}$ and $m_{2,2}$ does not imply consistency with $m_{0,4}$ because the incompressibility is not sufficient and knowledge of the pressure–gradient velocity–velocity structure function is required (Hill & Boratav 2001). An approximate relation between fourth-order statistics to estimate $m_{0,4}$ can be obtained by adopting the random sweeping hypothesis (Tennekes 1975) because the pressure–gradient velocity–velocity structure function can be disregarded. Since experiments do not support the random sweeping hypothesis (Hill & Boratav 2001), the consistency of the model with $m_{0,4}$ can not be derived. Finally, imposing $\{k = 3,\ n = 0\}$ to (5.13) gives

$$\rho = \frac{1}{m_{3,1}}\left[2m_{4,0} + \frac{r}{3}\frac{\partial m_{4,0}}{\partial r} + C_0\varepsilon r\frac{m_{3,0}}{m_{2,0}} - \frac{3}{2}m_{2,2}\right]. \tag{5.14}$$

In the next section, the Eulerian statistics $m_{k,n}$ needed to compute ρ and to determinate the drift a_i are determined by the analysis of the DNS data.

5.3. *DNS data analysis and drift determination*

5.3.1. *Universal constants and drift determination*

The universal constants $\{C_0, C_K\}$ and the unknown fourth-order Eulerian statistics $\{m_{4,0}, m_{2,2}, m_{3,1}\}$ computed from the corresponding Lagrangian or Eulerian dataset of the same DNS (Biferale *et al.* 2005), see table 1 and figures 2–3, are:

$$C_0 = 5, \quad C_K = \tfrac{7}{4}, \tag{5.15}$$

$$m_{4,0} = \tfrac{87}{8}(\varepsilon r)^{4/3}, \quad m_{2,2} = \tfrac{52}{5}(\varepsilon r)^{4/3}, \quad m_{3,1} = -\tfrac{31}{20}(\varepsilon r)^{4/3}. \tag{5.16}$$

The accepted values in literature are $C_0 = 5$ (Anfossi *et al.* 2000) and $C_K = 4.02 \times 0.5 = 2.01$ (Sreenivasan 1995). The longitudinal flatness value considered here is $m_{4,0}/m_{2,0}^2 = 174/49 \simeq 3.55$, even if a non-constant value of the flatness with respect to r is evident in figure 4. The flatness value increases when the Reynolds number increases (Antonia, Satyaprakash & Chambers 1982; Pearson & Antonia 2001). In

https://doi.org/10.1017/S0022112008003820 Published online by Cambridge University Press

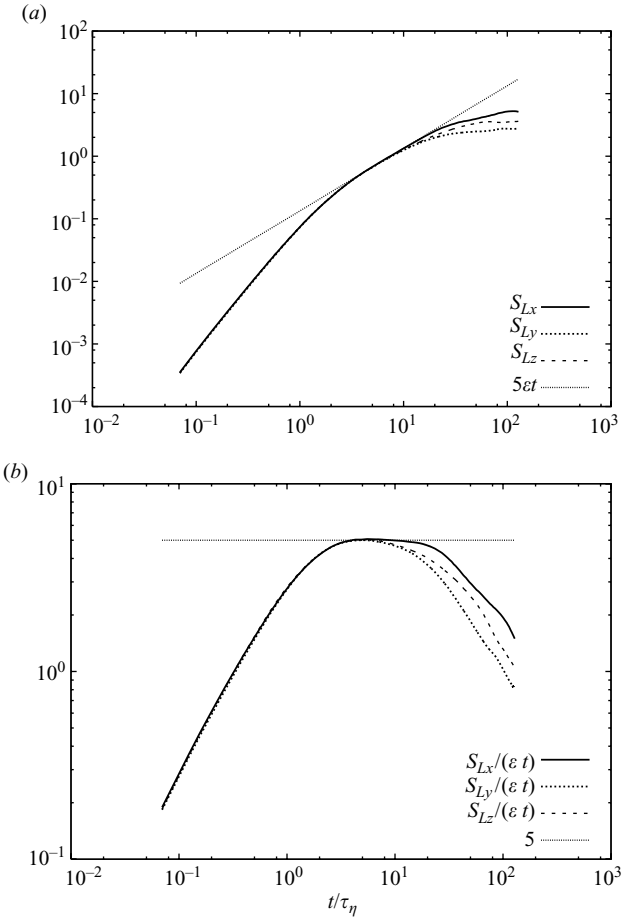


FIGURE 2. The second-order Lagrangian structure function in Cartesian coordinates $S_L = C_0\varepsilon t$ computed from the DNS data at $R_\lambda = 284$ (Biferale *et al.* 2005): $C_0 = 5$.

the literature, flatness values are found to be approximately 4 (see Antonia *et al.* 1982, 1997; Hill & Wilczak 1995, 2001).

Another important dimensionless fourth-order moment is the ratio $H = m_{2,2}/(2m_{4,0})$, because it is strongly related to the longitudinal pressure–gradient velocity–velocity structure function (Hill & Boratav 2001). From (5.16), $H = 208/435 \simeq 0.48$, which is in agreement with literature values. In fact, H is determined as $H = 5/9$, with the random sweeping approximation (Hill & Boratav 2001), or as $H = 4/9$, with the Ould-Rouis *et al.* (1996) approximation formula. Moreover, experiments give $H = 0.43$ (Hill & Wilczak 1995) and $H = 0.44r^{0.05}$ (Nelkin & Chen 1998).

Finally, from (5.14) and (5.16) the coupling constant is determined as $\rho = -3653/651 \sim -5.6$ and the drift term a_i becomes

$$a_i = \left(-\frac{u_\parallel}{\tau(r)} - \frac{7}{3}\frac{u_\parallel^2}{r} + \frac{1}{2}\frac{u_\perp^2}{r} - \frac{3653}{651}\frac{u_\parallel u_\perp}{r} \right) \frac{r_i}{r} + \frac{u_\parallel u_i}{r}. \tag{5.17}$$

5.3.2. *Evaluation of neglect of intermittency on the Markov model*

It is well known that the high-order Eulerian statistics are affected by intermittency and Reynolds-number dependence (Antonia *et al.* 1982; Frisch 1996; Pearson &

https://doi.org/10.1017/S0022112008003820 Published online by Cambridge University Press

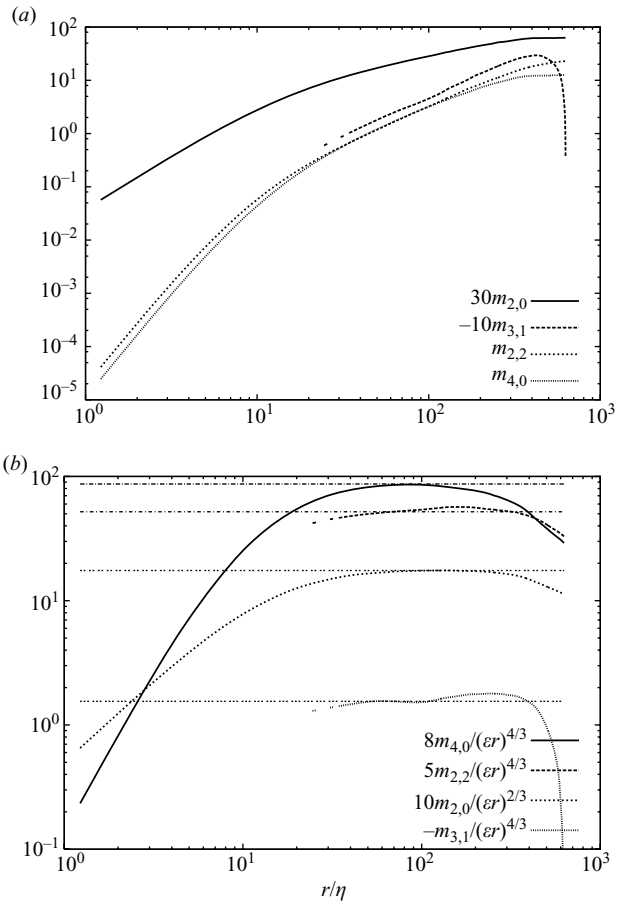


FIGURE 3. The Eulerian structure functions $m_{2,0}$, $m_{4,0}$, $m_{2,2}$, $m_{3,1}$ computed from the DNS data at $R_\lambda = 284$ (Biferale *et al.* 2005). (*b*) The horizontal lines correspond, from the top to the bottom, to the values: 87, 52, 35/2, 31/20.

Antonia 2001), and this effect is evident from the fourth order. However, the current model is non-intermittent so a measure of the departure from the K41 power law is important. Following (Hill & Wilczak 1995), in the inertial range

$$m_{4,0} = C_{4,0}\varepsilon^{4/3}r^q, \quad q = 4/3 - q', \tag{5.18}$$

where $C_{4,0}$ depends on the macrostructure of the flow and has the dimension of length raised to the power q'. This intermittency correction q' depends on the value of the intermittency parameter μ and the intermittency model adopted: from literature measurements, $\mu = 0.20$ (Sreenivasan & Kailasnath 1993) or 0.25 (Praskovsky & Oncley 1994), and from theory, $\mu = 2/9$ (She & Leveque 1994). Moreover, with the log-normal model $q' = 2\mu/9$ and then q' is 0.044 and 0.055 for the two experimental values of μ. With the β-model q' is equal to 0.067 and 0.083; the log-Poisson model $q' = 0.054$ (theoretical $\mu = 2/9$), the log-Lévy model $q' = 0.06$. For the definition of q' in the intermittency models see table 1 in Anselmet, Antonia & Danaila (2001), but note that there is a misprint. In fact, if in the log-Lévy model $\langle \varepsilon_r^p \rangle \sim (L/r)^{K(p)}$ then $m_{p,0} \sim r^{p/3}\langle \varepsilon_r^{p/3} \rangle \sim r^{p/3-K(p/3)}$ and so $\xi_p = p/3 - C_1[(p/3)^\varphi - (p/3)]/(\varphi - 1)$. From formula $\mu = 2 - \xi_6$ and the experimental

https://doi.org/10.1017/S0022112008003820 Published online by Cambridge University Press

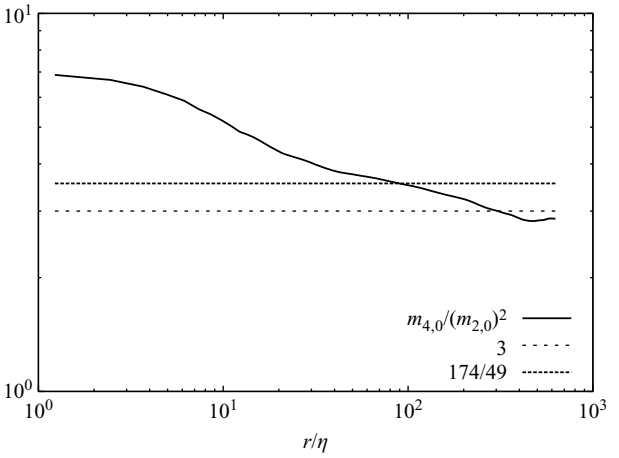


FIGURE 4. Eulerian longitudinal flatness $F = m_{4,0}/(m_{2,0})^2$ computed from the DNS data at $R_\lambda = 284$ (Biferale *et al.* 2005). Line $F = 3$ corresponds to a Gaussian density value while $F = 174/49$ is the flatness value obtained from (5.15)–(5.16) and considered in the present model.

measures $\{\varphi = 1.5, C_1 = 0.15\}$, the intermittency parameter is determined as $\mu \simeq 0.25$. With the misprinted formula $\xi_p = p/3 - C_1[p^\varphi - p]/(\varphi - 1)$, q' becomes 1.2 and $\mu \simeq 2.6$, which is too high when compared to the previous values. In conclusion, after this short review, disregarding the intermittency has little influence on the Markov model because very small differences from the 4/3 power law occur.

5.4. *Numerical results*

5.4.1. *Numerical simulation set-up*

The numerical simulations of the model are performed with the initial conditions $\{r_1 = r_2 = r_3 = r_0/\sqrt{3}\}$ and $\{u_1 = \sqrt{F}, u_2 = u_3 = \sqrt{G}\}$, where $\{r_i, u_i; i = 1, 3\}$ are the particle separation and the velocity difference in Cartesian coordinates, respectively, F is the longitudinal second-order structure function $F = C_K(\varepsilon r_0)^{2/3}$ and G the perpendicular one, which is determined as $G = 4F/3$ from the following formula (Monin & Yaglom 1975, p. 106):

$$\tfrac{1}{2}\langle u_\perp^2 \rangle = \langle u_\perp'^2 \rangle = \langle u_\parallel^2 \rangle + \frac{r}{2}\frac{\partial \langle u_\parallel^2 \rangle}{\partial r}. \tag{5.19}$$

Since the form of p_E is unknown, the initial velocity distribution does not meet the initial condition of (1.3). From this choice $r_i r_i = r_0^2$, $u_\parallel^2 = (u_i r_i/r)^2 = F$ and $u_\perp^2 = u_i u_i - u_\parallel^2 = 2G$. The initial separation is $r_0 = 2.4\eta$, and the time step $\mathrm{d}t$ is fixed at a value of $\mathrm{d}t = 10^{-5}$. The statistical moments are computed with 2000 particle pairs and the probability density functions by averaging 10 independent runs.

Moreover, Lagrangian stochastic model formulation requires the knowledge of some turbulent flow parameters, i.e ε, C_0, C_K. In particular, $\varepsilon = 0.81$ (see table 1) and $C_0 = 5$ and $C_K = 7/4$ (5.15).

5.4.2. *Particle separation density function*

Particle separation is described well in the inertial range by Richardson's (1926) suggestion. Later on, Richardson's ideas were formalized by Obukhov (1941) and

https://doi.org/10.1017/S0022112008003820 Published online by Cambridge University Press

t	$34.85\tau_\eta$	$55.77\tau_\eta$	$69.70\tau_\eta$
$\langle r\rangle$	0.69	1.38	1.93
$\langle r\rangle_{DNS}$	0.50	1.14	1.66
$\langle r^2\rangle$	0.56	2.25	4.40
$\langle r^2\rangle_{DNS}$	0.42	1.94	4.00
S	0.80	0.84	0.84
S_{DNS}	1.47	1.24	1.13
K	3.65	3.78	3.82
K_{DNS}	5.92	4.94	4.49

TABLE 3. Mean, variance, skewness $S = \langle(r-\langle r\rangle)^3\rangle/\langle(r-\langle r\rangle)^2\rangle^{3/2}$ and kurtosis $K = \langle(r-\langle r\rangle)^4\rangle/\langle(r-\langle r\rangle)^2\rangle^2$ of r computed by the PDF data of the model and DNS with $R_\lambda = 284$ at times: $34.85\tau_\eta$, $55.77\tau_\eta$, $69.70\tau_\eta$. For the Gaussian PDF $\{S_G = 0.5; K_G = 3.1\}$ and for the Richardson PDF $\{S_R = 1.7; K_R = 7.8\}$.

Batchelor (1950). In particular, the Richardson scheme is based on the idea of a spatial power law of the diffusion coefficient, i.e. $K(r) = \alpha r^{4/3}$ (Richardson 4/3 law). Inserting $K(r)$ into the diffusion equation the PDF of the particle separation gives

$$p_R(r;t) = 4\pi r^2 \frac{3}{35\pi^{3/2}} \left(\frac{3}{2}\right)^6 (\alpha t)^{-9/2} \exp\left\{-\frac{9r^{2/3}}{4\alpha t}\right\}, \tag{5.20}$$

which is called the Richardson density function. This probability density p_R is confirmed by experiments (Ott & Mann 2000) and DNS (Boffetta & Sokolov 2002; Yeung & Borgas 2004).

The comparison of the probability density of r among model (5.17), DNS, Gaussian and Richardson PDFs (5.20) is shown in figures 5 and 6 at three different time values, i.e. $t = 34.85\tau_\eta$, $t = 55.77\tau_\eta$ and $t = 69.70\tau_\eta$. In these plots, the PDFs are multiplied by $(\langle r^2\rangle - \langle r\rangle^2)^{1/2}$ and plotted against $(r - \langle r\rangle)/(\langle r^2\rangle - \langle r\rangle^2)^{1/2}$ to reduce the difference related to the specific numerical value of the moments as well as to highlight the scaling laws. This causes negative values in the abscissa. Since the viscous range is not modelled, the PDF of the model is quasi-Gaussian for low r, whereas a good scaling, close to that of the PDF of DNS, is observed for inertial range separation. However, in general, the particle separation density function generated by model (5.17) is not Gaussian (see table 3). The difference in the particle separation density functions at low r (figures 5–6) is generated by the different duration of the ballistic regime between the model and DNS (see also figures 7–9). In fact, strongly different physical conditions occur for low r. In the model, the viscous effects are completely neglected (the velocity initial condition is $F = C_K(\varepsilon r_0)^{2/3}$) whereas in DNS they are dominant because of the low Reynolds number ($F \sim r_0^2$).

This means that in DNS, when two particles are so close that they are in the viscous range, they require more time to return to an inertial range separation than particle pairs in the model. This causes a higher probability of finding a particle pair with small r in DNS than in the stochastic model. Furthermore, by increasing time towards the inertial range, the difference between the model and DNS decreases in all statistics, as can be seen in figures 5 and 6.

With a more complex model the viscous effects can be considered and therefore the small time and small separation behaviour can be correctly described, as highlighted in (Borgas & Yeung 2004) with a quasi-one dimensional approach and in (Heppe 1998) with a non-Markovian model.

https://doi.org/10.1017/S0022112008003820 Published online by Cambridge University Press

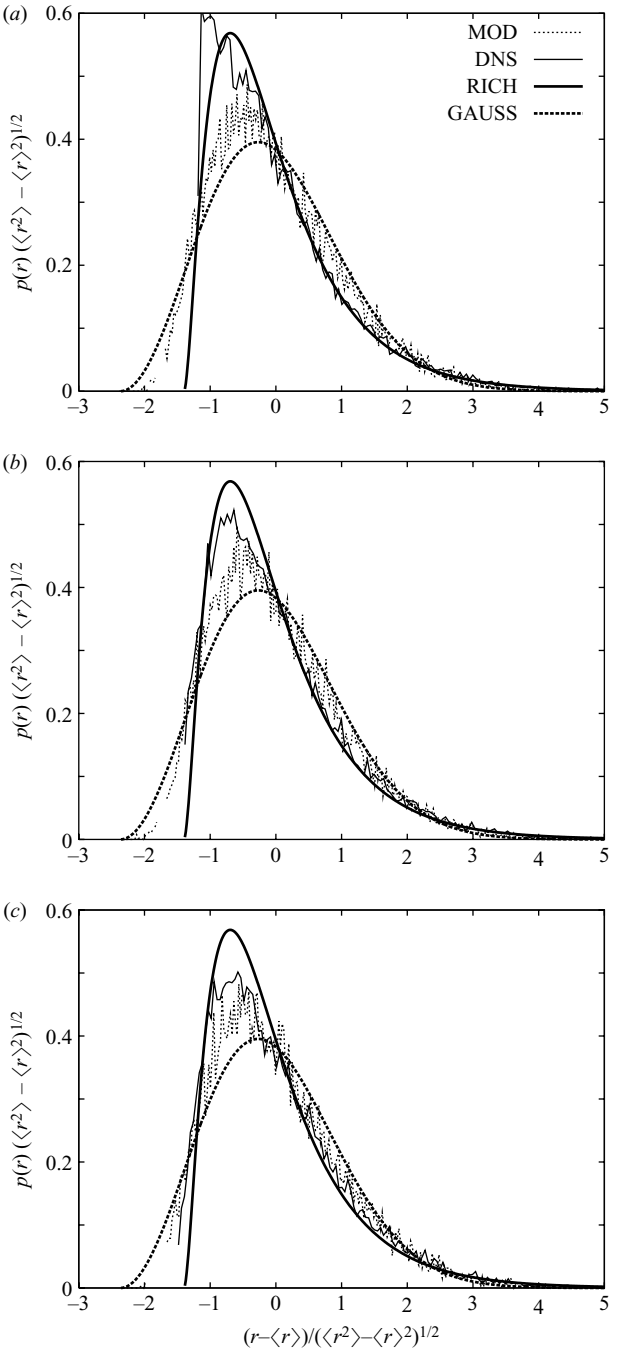


FIGURE 5. Comparison of the PDF of r among the model (MOD), DNS, Richardson PDF (RICH) and Gaussian PDF (GAUSS) at times $t = 34.85\tau_\eta$, $55.76\tau_\eta$, $69.70\tau_\eta$. The Reynolds number of DNS data is $R_\lambda = 284$ (Biferale *et al.* 2005).

https://doi.org/10.1017/S0022112008003820 Published online by Cambridge University Press

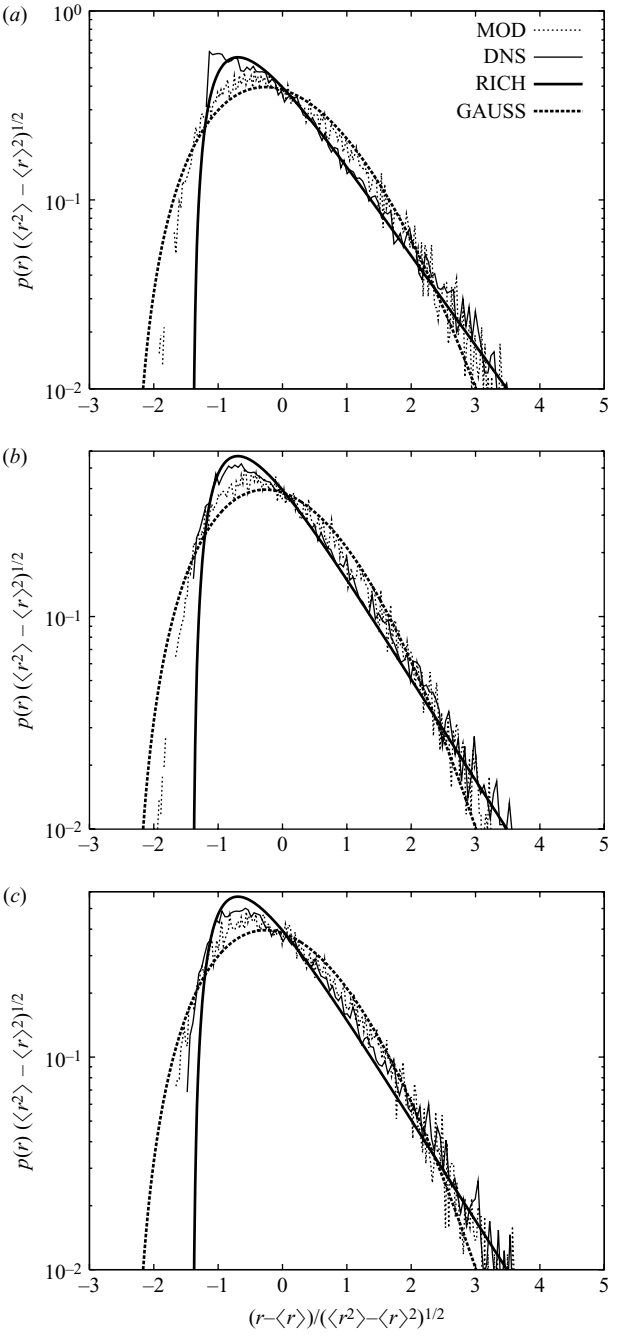


FIGURE 6. Comparison, on linear-log scales, of the PDF of r among the model (MOD), DNS, Richardson PDF (RICH) and Gaussian PDF (GAUSS) at times $t = 34.85\tau_\eta,\ 55.76\tau_\eta,\ 69.70\tau_\eta$. The Reynolds number of DNS data is $R_\lambda = 284$ (Biferale *et al.* 2005).

https://doi.org/10.1017/S0022112008003820 Published online by Cambridge University Press

5.4.3. *Particle separation statistics*

When the variance of the particle separation $\langle r^2 \rangle$ is computed using p_R (5.20), the so-called Richardson t^3 law is obtained

$$\langle r^2 \rangle = g\varepsilon t^3, \tag{5.21}$$

where $g = \varepsilon^{-1}(143/3)(2\alpha/3)^3$ is a universal constant. The value of the Richardson constant g ranges between 0.06 and 6 (Ott & Mann 2000). Experimental measurements by Ott & Mann (2000) and DNS (Boffetta & Sokolov 2002) give $g = 0.5$, and Berg *et al.* (2006) experimentally found $g = 0.55 \pm 0.05$. Moreover, with extrapolation to the large-Reynolds-number limit, Sawford, Yeung & Hackl (2008) obtained by the analysis of several DNS datasets, $g = 0.55 - 0.57$. In the inertial range, neglecting intermittency, from the dimensional analysis, $\langle r^n \rangle = g_n \varepsilon^{n/2} t^{3n/2}$, where g_n are universal constants and $g_2 = g$ is the Richardson constant. An important feature of Lagrangian models is their ability to reproduce the t^3 law (5.21) with a value of g in agreement with the experimental and DNS literature value.

Figures 7, 8 and 9 show the plots of the mean separation $\langle r \rangle$, the root mean square separation $\langle r^2 \rangle^{1/2}$ and the mean square separation $\langle r^2 \rangle$, respectively. The model and DNS are compared with respect to the ballistic and inertial scalings and the fits shown in the plots are those with the corresponding universal constants. In these figures, the inertial range dimensional behaviour of the model statistics is evident, whereas that of DNS is affected by low-Reynolds-number and viscous effects. In particular, in figure 7, constant g_1 is fitted as $g_1 = 0.6$ and, in figure 9, the Richardson constant of the Lagrangian model and that of DNS are very close and the value $g = 0.43$ has been taken. This value is in better agreement with experimental (Ott & Mann 2000; Berg *et al.* 2006) and DNS (Boffetta & Sokolov 2002; Ishihara & Kaneda 2002) literature values than other stochastic models, see § 5.5.1 and table 4.

A difference between the model and DNS after the ballistic regime is evident in figures 7, 8 and 9. However, comparing this discrepancy for $\langle r^2 \rangle^{1/2}$ and $\langle r \rangle$, which from the above non-intermittent dimensional analysis have the same power law, it is clearly less for $\langle r^2 \rangle^{1/2}$ (figure 8) than for $\langle r \rangle$ (figure 7). This suggests different scalings and may be the result of intermittency effects. In fact, as Novikov (1989) pointed out, $\langle r^2 \rangle$ is the only statistic not affected by intermittency corrections. This can also be the explanation for the good performance of the Markov model to capturing $\langle r^2 \rangle$, even if the DNS data are intermittent.

An important test for the model is to verify its ability to reproduce the t^3 law, with a Richardson constant g in agreement with the literature value, even in standard case studies which are not related to the particular DNS dataset by Biferale *et al.* (2005). Details of this analysis are presented in Appendix C. It follows that for $C_K = 2.1$, as suggested by Sreenivasan (1995), and $C_0 = 5$, 6 and 7, the values of g obtained are 0.45, 0.55 and 0.65, respectively. Moreover, setting $C_K = 2$ and $C_0 = 6$, in both case studies $\sigma_{1_p}^2 = \varepsilon = 1$ and $\tau_L = \lambda = 1$, the Richardson constant turns out to be 0.55. These results show a very good agreement of the model with the experimentally measured Richardson constant $g = 0.55 \pm 0.05$ by Berg *et al.* (2006) and with the extrapolation to the large-Reynolds-number limit $g = 0.55 - 0.57$ derived by Sawford *et al.* (2008).

5.5. *Performance comparison with other models*

5.5.1. *The value of the Richardson constant*

After the comparisons with other well-mixed models, with respect to the theoretical formulation, now the model performances are compared with respect to the value of

https://doi.org/10.1017/S0022112008003820 Published online by Cambridge University Press

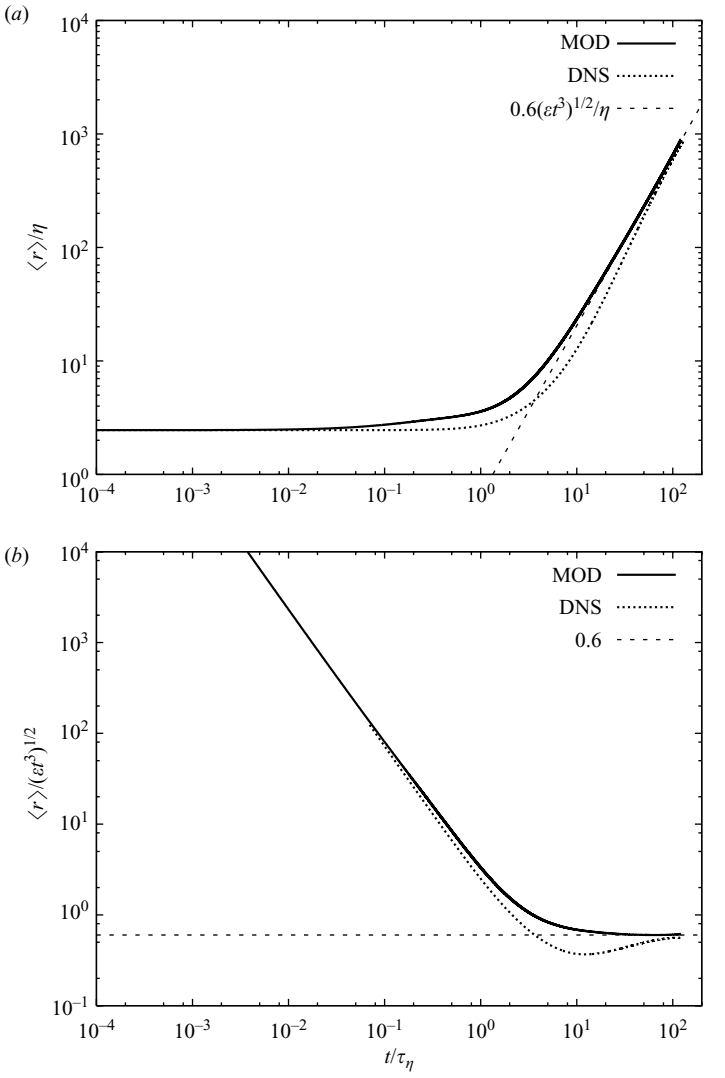


FIGURE 7. Comparison between the model (MOD) and DNS of the ballistic and inertial scalings of $\langle r\rangle$. The dotted straight line is the fit in the inertial range of the universal constant that emerges from dimensional analysis. The Reynolds number of DNS data is $R_\lambda = 284$ (Biferale *et al.* 2005).

the Richardson constant g. For this purpose, moments approximated models are also included (Pedrizzetti & Novikov 1994; Heppe 1998). In the present study, a good fit of the DNS data and the model is found for $g = 0.43$. The reference literature value is $g \sim 0.5$ (Ott & Mann 2000; Boffetta & Sokolov 2002; Ishihara & Kaneda 2002; Berg *et al.* 2006).

Since Lagrangian stochastic models in the well-mixed class depend on a dimensionless parameter β, which is the Lagrangian-to-Eulerian scale ratio (Maurizi, Pagnini & Tampieri 2004, 2006), the comparison of performances is done with the same value of β for all models. This parameter β can be related to the universal constants C_0 and C_K in the following way. Let S_L and S_E be the second-order structure

https://doi.org/10.1017/S0022112008003820 Published online by Cambridge University Press

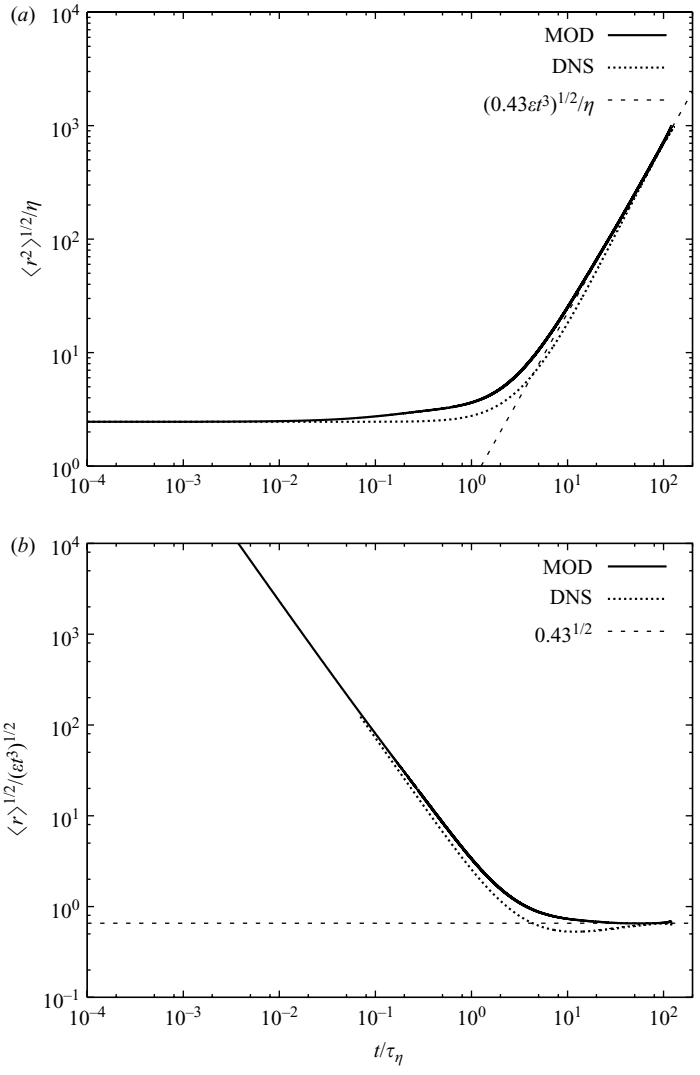


FIGURE 8. As figure 7, but for scalings of $\langle r^2\rangle^{1/2}$.

functions in the Lagrangian and in the Eulerian frame, respectively, given by

$$S_L = 2\,\sigma_{1p}^2\, t/\tau_L = C_0\varepsilon t, \quad S_E = 2\,\sigma_{1p}^2\,(r/\lambda)^{2/3} = C_K(\varepsilon r)^{2/3},$$

where τ_L denotes the Tennekes Lagrangian time scale defined by (4.18). A similar definition for Eulerian length scale (Maurizi *et al.* 2004, 2006)

$$\lambda = \varepsilon^{-1}\left(\frac{2\sigma_{1p}^2}{C_K}\right)^{3/2} \tag{5.22}$$

follows. From (5.15), table 1 and $\sigma_{1p}^2 = u_{rms}^2$, the length scale λ is determined to be $\lambda = 7.41$. Combining (4.18) and (5.22) the dimensionless parameter β can be expressed

https://doi.org/10.1017/S0022112008003820 Published online by Cambridge University Press

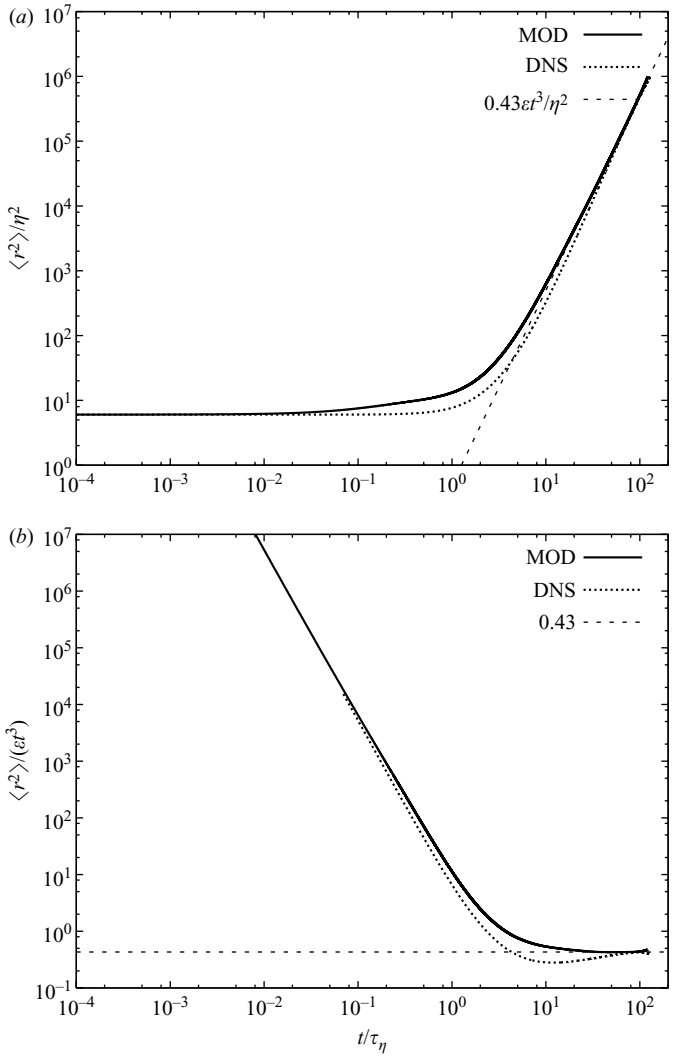


FIGURE 9. Comparison between the model (MOD) and DNS of the ballistic and inertial scalings of $\langle r^2\rangle$. The dotted straight line is the fit in the inertial range of the Richardson constant: $g = 0.43$. The Reynolds number of DNS data is $R_\lambda = 284$ (Biferale *et al.* 2005).

as

$$\beta = \frac{\sigma_{1p}\,\tau_L}{\lambda} = \frac{C_K^{3/2}}{\sqrt{2}C_0}. \tag{5.23}$$

To perform numerical simulations of model (5.17) the value of β must be determined. This requires β to be computed with Eulerian and Lagrangian quantities measured in the same experiment or DNS. From the DNS data analysed, the parameter β is determined as $\beta = (7/4)^{3/2}/(5\sqrt{2}) \sim 0.33$. Eulerian and Lagrangian quantities from the same experiment or DNS seems to be unavailable in literature as yet. Moreover, Eulerian and Lagrangian parameters measured by the same DNS are not used to construct models in the intercomparisons between stochastic models and DNS (Heppe 1998; Borgas & Yeung 2004). It is important to remark that here, differently from

https://doi.org/10.1017/S0022112008003820 Published online by Cambridge University Press

Models	g	C_K	C_0	β
Present model (DNS comparison)	0.43	7/4	5	0.33
Present model (standard case study, Appendix C)	0.55	2	6	0.33
Well-mixed models with Gaussian PDF				
Borgas & Sawford (1994):				
Model (4.2*a*)	0.6	2	6	0.33
Model (4.3)	1.16	2	6	0.33
Model (7.6) with $\varphi = -0.4$	0.9	2	6	0.33
Thomson (1990)	1.1	2	6	0.33
Quasi-one-dimensional well-mixed models				
Borgas & Yeung (1998)	1.7	2	6	0.33
Kurbanmuradov *et al.* (2001):				
Bi-Gaussian PDF ($\sigma_1 = \sigma_2$)	1.67	2	6	0.33
Bi-Gaussian PDF ($\mu_1/\sigma_1 = -\mu_2/\sigma_2$)	2.27	2	6	0.33
Gaussian PDF	2.8	2	6	0.33
Sawford *et al.* (2005):				
Tri-Gaussian PDF (1, 0.929)	1.14	2	7	0.29
Moments approximated models				
Pedrizzetti & Novikov (1994) ($c = 9.5$, $\gamma = 3$)	0.122	2	7.1	0.28
Heppe (1998)	0.44	2	16/3	0.37

TABLE 4. The g values of Borgas & Sawford (1994) are taken from the data file of figure 2 in Maurizi *et al.* (2006), the other values from Kurbanmuradov *et al.* (2001) except those from Pedrizzetti & Novikov (1994) and Sawford *et al.* (2005), which are taken from the original papers. For the meaning of the model parameters please refer to the original papers.

previous model–DNS intercomparisons (Heppe 1998; Borgas & Yeung 2004), the Eulerian statistics used are those measured from the same DNS as the Lagrangian statistics and not literature values. The comparison of the values of the Richardson constant obtained with the present and other models for $\beta \sim 0.33$ are shown in table 4.

The comparison with Pedrizzetti (1999) and Borgas & Yeung (2004) models is not included. In particular, the comparison with the Pedrizzetti (1999) model is not shown in table 4, because the β value in the original paper is not comparable; however, for the same model in Kurbanmuradov *et al.* (2001) it is shown that $g = 0.35$ when $\beta = 0.2$ ($C_K = 2$, $C_0 = 10.25$). Also, the comparison with Borgas & Yeung (2004) is not possible because they have $\beta = 0.23$ ($C_K = 2.1$, $C_0 = 9$) and, furthermore, because their results are the consequence of the collective choice of a number of free parameters tuned for optimal agreement with their DNS data. Here, the good agreement with the DNS g value follows from no free tunable parameter.

From the analysis of table 4, it follows that, even if qualitatively in agreement with the DNS data, the quasi-one-dimensional model, predicts higher value of g. The same conclusion is reported in Kurbanmuradov *et al.* (2001). Moreover, for what concerns the tri-Gaussian quasi-one-dimensional model (Kurbanmuradov 1997), besides the value of g given in Sawford *et al.* (2005) and reported in table 4, we can estimate from figure 2(*a*) in Sawford *et al.* (2005) that $g \sim 2$ when $\beta = 0.33$ ($C_K = 2$, $C_0 = 6$) for both couples of parameters (0.2, 0.827) and (1, 0.929).

A comparison similar to the present is made by Reynolds (1999*b*) using a one-dimensional and a quasi-one-dimensional model with Gaussian and maximum missing information (MMI) density functions. Unfortunately, this study uses $\beta = 1$ ($C_K = C_0 = 2$). However, he observes an overestimation of g by the quasi-one-dimensional model. In fact, for the one-dimensional model, $g = 1.26$ (Gaussian PDF) and $g = 0.56$

https://doi.org/10.1017/S0022112008003820 Published online by Cambridge University Press

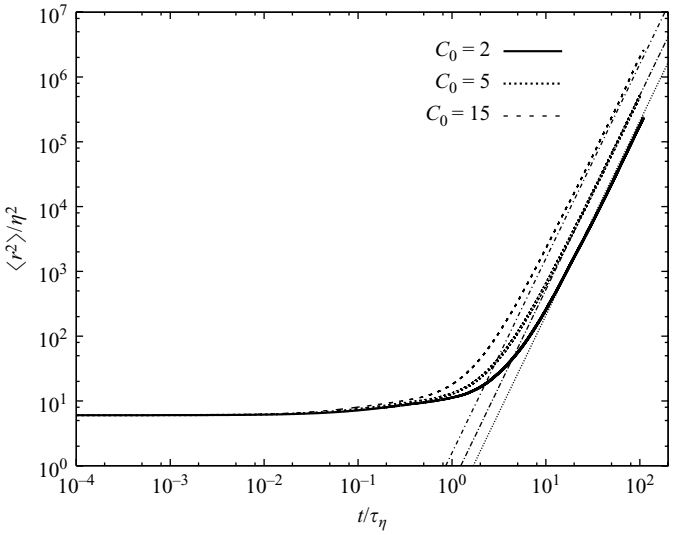


FIGURE 10. The model agreement with the Franzese–Cassiani formula (5.24) for three different values of C_0 (2, 5, 15) and the predicted values of g (0.18, 0.45, 1.36).

(MMI PDF); for the quasi-one-dimensional model, $g = 13.6$ (Gaussian PDF) and $g = 1.0$ (MMI PDF).

Finally, with regard to the Richardson constant, it can be said that, generally, the present model is in better agreement with the literature value than other models. The same good agreement occurs with the Gaussian well-mixed model by Borgas & Sawford (1994) called 'model (4.2*a*)' and the moments approximated model by Heppe (1998).

5.5.2. *The consistency with the Franzese–Cassiani formula*

An important and surprising result of the present model is the excellent agreement with the recent statistical theory of turbulent relative dispersion by Franzese & Cassiani (2007). They theoretically derived the following formula (formula (8.1) in their paper):

$$g = (18\sqrt{6} - 44)C_0. \tag{5.24}$$

To compare the model with the Franzese–Cassiani formula (5.24), parameter ρ (5.14) has to be computed for different values of C_0 and C_K. Formula (5.23) yields

$$C_K = (\sqrt{2}C_0\beta)^{2/3},$$

where β can be considered a 'universal constant' when expressed in terms of the universal constants C_0 and C_K (5.23). In this case, β must be fixed for every $\{C_0, C_K\}$ pair and, in particular, from the DNS data analysed, β is equal to $(7/4)^{3/2}/(5\sqrt{2}) \sim 0.33$. Subsequently, taking this 'universal' value of β, for every simulation, the values of C_K and ρ are given by

$$C_K = \frac{7}{4}\left(\frac{C_0}{5}\right)^{2/3}, \quad \rho = -\frac{4613 - 960(C_0/5)^{1/3}}{651},$$

with $C_K = 7/4$ and $\rho = -3653/651$ when $C_0 = 5$. The agreement with (5.24) is shown in figure 10 where $\langle r^2 \rangle$ is plotted for three different values of C_0 (2, 5, 15) and compared with the three predictions of g (0.18, 0.45, 1.36).

https://doi.org/10.1017/S0022112008003820 Published online by Cambridge University Press

6. Discussion and conclusions

It is well known that there is important non-uniqueness in two-particle Markovian stochastic models of dispersion (Borgas & Sawford 1994). Despite this, a valid application of the stochastic-model approach for describing Lagrangian statistics in turbulent flow can be found in Borgas & Yeung (2004). They show that stochastic models, when properly formulated, are efficient representations of the turbulent dispersion process. Moreover, the non-Markovian aspect related to the viscous range can be modelled well (see Heppe 1998).

The present paper is focused on the non-uniqueness problem. Starting from turbulent flows being rotational, the physical picture of a fluid particle pair as a couple of material points rotating around their centre of mass is proposed to model turbulent relative dispersion in the inertial range. Coupling this physical picture with the well-mixed condition, a way to kinematically construct the acceleration field is obtained, leading to a constraint for the non-uniqueness problem.

The formulation proposed is based on the particle pair rotation that is represented with an explicit angular velocity derived from two-particle mechanics. This angular velocity is an important element for the consistency of the derived stochastic process with some turbulent-flow characteristics, especially in comparison with previous formulations. In particular, it is consistent with the following characteristics: (i) the statistical dependence between the longitudinal and orthogonal components of the velocity difference vector; (ii) the non-null vorticity field; and (iii) the small-length-scale limit and the large-fluctuation regime. The first characteristic is a fundamental aspect of the Navier–Stokes equations that, instead, is not satisfied by the Kurbanmuradov quasi-one-dimensional assumption closure scheme and by the non-unique Gaussian models. In the formulation proposed, the above property is due to the non-null angular velocity, but, notwithstanding this, its effects on the mean rotation are null and the isotropy is preserved. Furthermore, the consistency with the Navier–Stokes equations is observed also in respect of a non-null vorticity field. In fact, it is shown that the non-zero angular velocity of the particle pair preserves a non-null vorticity field. This also means that every model with a zero angular velocity is not consistent with a non-null vorticity field. Finally, the small-length-scale limit and the large-fluctuation regime are analysed and the formulation proposed is better than the previous ones. In particular, the quasi-one-dimensional-approach models cannot be reduced to the small-length-scale limit and, moreover, when based on the quasi-one-dimensional assumption, they cannot be formulated in the large-fluctuation regime because of the non-factorizable Eulerian density. The non-unique Gaussian models do not satisfy the large-fluctuation regime.

A simple Markov model is also developed as a merely illustrative application of the formulation proposed. The viscous range is not modelled to avoid introducing complexity, physical approximations and free parameters, and to highlight the inertial range behaviour. Despite its simplicity, in the inertial range, the model is consistent with more Eulerian statistical moments than previous models in literature and a good agreement is observed with DNS data both for statistics and probability density function of particle separation. Moreover, the comparison on the value of the Richardson constant g with several models clearly shows that the model proposed performs better than the others and it is at the same level as the Gaussian well-mixed model by Borgas & Sawford (1994) called 'model (4.2a)' and the moments approximated model by Heppe (1998). In particular, the value of the Richardson constant g is equal to 0.43, in agreement with the literature value. Finally, the present

https://doi.org/10.1017/S0022112008003820 Published online by Cambridge University Press

model turns out to be in agreement with the formula to relate g and C_0 derived by Franzese & Cassiani (2007).

Recall that all the good performances of the model are obtained without any free tunable parameters. This remarkable fact supports the formulation proposed. However, it must be remarked also that the model parameter ρ (5.14) is determined using values of the constant factors of some Eulerian statistics (5.15) and (5.16) computed by the same DNS dataset considered for the comparison. This means that, in principle, in order to have a consistent comparison with another DNS dataset, the parameter ρ must be re-computed. In fact, different values of the constant factors of the Eulerian statistics can occur, expecially for DNS datasets with distinct Reynolds numbers, and then a different value of the parameter ρ follows. With respect to this issue, also some standard case studies are analysed to test the model performances in situations independent of the DNS dataset by Biferale *et al.* (2005). In these cases, the Richardson constant of the model ranges from 0.45 to 0.65. In particular, setting $C_K = 2.1$ and $C_0 = 6$, or in both case studies $\sigma_{1_p}^2 = \varepsilon = 1$ and $\tau_L = \lambda = 1$ with $C_K = 2$ and $C_0 = 6$, the Richardson constant turns out to be 0.55, which is in very good agreement with the experimental measure $g = 0.55 \pm 0.05$ (Berg *et al.* 2006) and the estimation $g = 0.55 - 0.57$ by Sawford *et al.* (2008). The model performs very well also in standard situations and not only when compared with the DNS data by Biferale *et al.* (2005). This last result is an independent positive confirmation of the model and the formulation proposed.

The author gratefully acknowledges F. Tampieri and A. Maurizi for their continuous support, fruitful discussions and suggestions all through the period of the realization of the work; A. Celani for advice and comments during the two visits to INLN-CNRS (Nice, France); G. Boffetta and A. Lanotte for the DNS data, and the supercomputing centre CINECA (Bologna, Italy) http://cfd.cineca.it for housing them; the University of Bologna for the financial support to the second research period at INLN-CNRS via 'Programma Marco Polo VIII'. The author would also like to thank R. A. D. Akkermans at Eindhoven University of Technology, P. Buttol and L. Ferri at ENEA for carefully reading the manuscript.

Appendix A. Kinematics in the rotational case

A.1. *Angular momentum and angular velocity*

In mechanics, the rotation around a point is the consequence of a non-zero angular momentum $\boldsymbol{M}$, which is defined for a particle with unitary mass as (Landau & Lifshitz 1960, p. 19)

$$\boldsymbol{M} = \boldsymbol{d} \times \dot{\boldsymbol{d}}, \tag{A 1}$$

where $\boldsymbol{d}$ is the separation between the particle and the point and $\dot{\boldsymbol{d}} = \mathrm{d}\boldsymbol{d}/\mathrm{d}t$. The angular velocity $\boldsymbol{\Theta}$ is defined as (Landau & Lifshitz 1960, p. 106)

$$M_i = I_{ik}\Theta_k, \tag{A 2}$$

where $I_{ik} = d^2\delta_{ik} - d_i d_k$ is the inertial momentum tensor (Landau & Lifshitz 1960, p. 99). Generally, when the particle moves, the modulus and the direction of $\boldsymbol{\Theta}$ change. Moreover, $\boldsymbol{M}$ and $\boldsymbol{\Theta}$ usually have different directions, except in the special cases when the rotation occurs around one of the symmetry axes (Landau & Lifshitz 1960, p. 106). One of these special cases is that of a solid line. Such a system is called a rotator. The

https://doi.org/10.1017/S0022112008003820 Published online by Cambridge University Press

characteristic property which distinguishes a rotator from other bodies is that it has only two, not three, rotational degrees of freedom, corresponding to rotations about the two axes perpendicular to the solid line: it is clearly meaningless to speak of the rotation of a straight line about itself (Landau & Lifshitz 1960, p. 101). In this special case, the inertial momentum tensor I_{ik} becomes a diagonal matrix with $I_{ii} = d^2$ and $I_{ik} = 0$ for $i \neq k$, then from (A 2)

$$\boldsymbol{M} = d^2 \boldsymbol{\Theta}. \tag{A 3}$$

The combination of (A 1) and (A 3) gives

$$\boldsymbol{\Theta} = \frac{1}{d^2}(\boldsymbol{d} \times \dot{\boldsymbol{d}}). \tag{A 4}$$

However, formulae (A 3) and (A 4) hold also in the case of a particle whose translational motion occur only radially with respect to a point. In fact, it is similar to the following situations: (*a*) a sequence of particles along a solid body line rotating around one of its two extremes and at any instant t only the particle located in $\boldsymbol{d}(t)$ is considered, or (*b*) a particle forced to move along a solid line track rotating around one of its two extremes and at time t the particle is located at distance $\boldsymbol{d}(t)$ from the fixed extreme. In other words, the positional vector of a particle that can move only radially along a line in two different instants defines a plane, a rotational angle θ, a rotational axis perpendicular to the plane, and an angular velocity $\boldsymbol{\Theta} = \mathrm{d}\theta/\mathrm{d}t$ aligned with the rotational axis. This rotational axis is then perpendicular to the positional vector, i.e. $\boldsymbol{\Theta} \perp \boldsymbol{d}$.

A.2. *The Lagrangian relative velocity*

In the case of relative dispersion of two fluid particles, the centre of mass of the system can be considered as the origin of a non-inertial reference frame, where $\boldsymbol{r}^{CM} = (\boldsymbol{r}^{(1)} + \boldsymbol{r}^{(2)})/2$ and $\boldsymbol{u}^{CM} = (\boldsymbol{u}^{(1)} + \boldsymbol{u}^{(2)})/2$ are its position and its velocity, respectively. The three-dimensional separation $\boldsymbol{r} = \boldsymbol{r}^{(1)} - \boldsymbol{r}^{(2)}$ is an axis of this reference frame. By definition, the centre of mass falls on the line joining the two particles for all times. Since each particle can move only radially in this frame, it is possible to apply the previous arguments. The velocity vector of the particles is

$$\boldsymbol{u}^{(i)} = \boldsymbol{u}^{CM} + \boldsymbol{V}^{(i)},$$

where $\boldsymbol{V}^{(i)}$ is the i-particle velocity in the non-inertial system. The particles considered are fluid particles and not material points of a solid body, therefore their translational motion in the non-inertial frame is non-zero. As a consequence, their motion is the sum of a translational $\boldsymbol{V}_T^{(i)}$ and a rotational $\boldsymbol{V}_R^{(i)}$ component, i.e. $\boldsymbol{V}^{(i)} = \boldsymbol{V}_T^{(i)} + \boldsymbol{V}_R^{(i)}$. If the origin of the non-inertial frame is the centre of mass of the two particles, the particles can move only radially along $\boldsymbol{r}$ and the translation velocity is $\boldsymbol{V}_T^{(i)} = (u_\parallel^{(i)} - u_\parallel^{CM})\boldsymbol{r}/r$. The rotational part is $\boldsymbol{V}_R^{(i)} = \boldsymbol{\Omega}^{(i)} \times (\boldsymbol{r}^{(i)} - \boldsymbol{r}^{CM})$, where $\boldsymbol{\Omega}^{(i)}$ is the angular velocity. Finally,

$$\boldsymbol{u}^{(i)} = \boldsymbol{u}^{CM} + \left(u_\parallel^{(i)} - u_\parallel^{CM}\right)\frac{\boldsymbol{r}}{r} + \boldsymbol{\Omega}^{(i)} \times \left(\boldsymbol{r}^{(i)} - \boldsymbol{r}^{CM}\right). \tag{A 5}$$

From (A 5), the velocity of each particle is

$$\begin{aligned} \boldsymbol{u}^{(1)} &= \boldsymbol{u}^{CM} + \left(u_\parallel^{(1)} - u_\parallel^{CM}\right)\frac{\boldsymbol{r}}{r} + \boldsymbol{\Omega}^{(1)} \times \left(\boldsymbol{r}^{(1)} - \boldsymbol{r}^{CM}\right) \\ &= \boldsymbol{u}^{CM} + \left(u_\parallel^{(1)} - u_\parallel^{CM}\right)\frac{\boldsymbol{r}}{r} + \boldsymbol{\Omega}^{(1)} \times \frac{\boldsymbol{r}}{2}, \end{aligned} \tag{A 6}$$

https://doi.org/10.1017/S0022112008003820 Published online by Cambridge University Press

$$\begin{aligned}\boldsymbol{u}^{(2)} &= \boldsymbol{u}^{CM} + \left(u_{\parallel}^{(2)} - u_{\parallel}^{CM}\right)\frac{\boldsymbol{r}}{r} + \boldsymbol{\Omega}^{(2)} \times \left(\boldsymbol{r}^{(2)} - \boldsymbol{r}^{CM}\right) \\ &= \boldsymbol{u}^{CM} + \left(u_{\parallel}^{(2)} - u_{\parallel}^{CM}\right)\frac{\boldsymbol{r}}{r} - \boldsymbol{\Omega}^{(2)} \times \frac{\boldsymbol{r}}{2}. \end{aligned} \tag{A 7}$$

Since $\boldsymbol{r}^{(1)} - \boldsymbol{r}^{CM} = \boldsymbol{r}/2$ and $\boldsymbol{r}^{(2)} - \boldsymbol{r}^{CM} = -\boldsymbol{r}/2$ are used, different signs in front of the rotational component of (A 6) and (A 7) result.

In the centre-of-mass frame, the translational movement of the particles is always radial along line $\boldsymbol{r}$, therefore the previous arguments (A 1)–(A 4) can be applied with $\boldsymbol{d}^{(i)} = \boldsymbol{r}^{(i)} - \boldsymbol{r}^{CM}$ so that $\boldsymbol{d}^{(1)} = -\boldsymbol{d}^{(2)} = \boldsymbol{r}/2$ and $d^2 = r^2/4$. From (A 4), the angular velocity of each particle is

$$\boldsymbol{\Omega}^{(i)} = \frac{4}{r^2}\left[\left(\boldsymbol{r}^{(i)} - \boldsymbol{r}_{CM}\right) \times \left(\boldsymbol{u}^{(i)} - \boldsymbol{u}_{CM}\right)\right]. \tag{A 8}$$

Substituting $\boldsymbol{u}^{(1)} - \boldsymbol{u}_{CM} = \boldsymbol{u}/2$ and $\boldsymbol{u}^{(2)} - \boldsymbol{u}_{CM} = -\boldsymbol{u}/2$ in (A 8) gives

$$\begin{aligned}\boldsymbol{\Omega}^{(1)} = \boldsymbol{\Omega}^{(2)} &= \frac{4}{r^2}\left(\frac{\boldsymbol{r}}{2} \times \frac{\boldsymbol{u}}{2}\right) \\ &= \frac{1}{r^2}(\boldsymbol{r} \times \boldsymbol{u}). \end{aligned} \tag{A 9}$$

Finally, from (A 5)–(A 9), the Lagrangian relative velocity can be written as

$$\begin{aligned}\boldsymbol{u} &= \boldsymbol{u}^{(1)} - \boldsymbol{u}^{(2)} \\ &= \left(u_{\parallel}^{(1)} - u_{\parallel}^{(2)}\right)\frac{\boldsymbol{r}}{r} + \left(\boldsymbol{\Omega}^{(1)} + \boldsymbol{\Omega}^{(2)}\right) \times \frac{\boldsymbol{r}}{2} \\ &= u_{\parallel}\frac{\boldsymbol{r}}{r} + \frac{1}{r^2}(\boldsymbol{r} \times \boldsymbol{u}) \times \boldsymbol{r} \\ &= u_{\parallel}\frac{\boldsymbol{r}}{r} + \boldsymbol{\Omega} \times \boldsymbol{r}, \end{aligned} \tag{A 10}$$

where

$$\boldsymbol{\Omega} = \frac{1}{r^2}(\boldsymbol{r} \times \boldsymbol{u}). \tag{A 11}$$

Appendix B. Proof of (3.23)

Taking the time derivative of (3.1) gives

$$\boldsymbol{A} = \frac{\mathrm{d}\boldsymbol{u}}{\mathrm{d}t} = \left(A_{\parallel} + \frac{u_{\perp}^2}{r}\right)\frac{\boldsymbol{r}}{r} + \boldsymbol{\Omega} \times \boldsymbol{u} + \frac{u_{\parallel}}{r}\boldsymbol{u} - \frac{u_{\parallel}^2}{r}\frac{\boldsymbol{r}}{r} + \dot{\boldsymbol{\Omega}} \times \boldsymbol{r}, \tag{B 1}$$

where, if (3.2) holds,

$$\dot{\boldsymbol{\Omega}} = \frac{\mathrm{d}\boldsymbol{\Omega}}{\mathrm{d}t} = \frac{1}{r^2}\left[(\boldsymbol{r} \times \boldsymbol{A}) - 2\frac{u_{\parallel}}{r}(\boldsymbol{r} \times \boldsymbol{u})\right]. \tag{B 2}$$

It is possible to show for substitution that, when (3.1) and (3.2) hold, a solution of (3.4) is

$$\boldsymbol{A} = \left(A_{\parallel} + \frac{u_{\perp}^2}{r}\right)\frac{\boldsymbol{r}}{r} + \boldsymbol{\Omega} \times \boldsymbol{u}. \tag{B 3}$$

This means that the following formula must be proved

$$\dot{\boldsymbol{\Omega}} \times \boldsymbol{r} + \frac{u_{\parallel}}{r}\boldsymbol{u} - \frac{u_{\parallel}^2}{r}\frac{\boldsymbol{r}}{r} = 0. \tag{B 4}$$

https://doi.org/10.1017/S0022112008003820 Published online by Cambridge University Press

Before starting the proof of (B 4), the following formulae are reminded

$$\boldsymbol{p}\times\boldsymbol{q}=-\boldsymbol{q}\times\boldsymbol{p},\quad \boldsymbol{p}\times(\boldsymbol{q}\times\boldsymbol{p})=\boldsymbol{q}\,(\boldsymbol{p}\cdot\boldsymbol{p})-\boldsymbol{p}\,(\boldsymbol{q}\cdot\boldsymbol{p}),$$

where $\boldsymbol{p}$ and $\boldsymbol{q}$ are two generic vectors, $u^2=\boldsymbol{u}\cdot\boldsymbol{u}=u_\parallel^2+u_\perp^2$, and

$$\begin{aligned}\boldsymbol{\Omega}\times\boldsymbol{u}=\frac{1}{r^2}(\boldsymbol{r}\times\boldsymbol{u})\times\boldsymbol{u}&=-\frac{1}{r^2}\boldsymbol{u}\times(\boldsymbol{r}\times\boldsymbol{u})\\&=-\frac{1}{r^2}[\boldsymbol{r}\,(\boldsymbol{u}\cdot\boldsymbol{u})-\boldsymbol{u}\,(\boldsymbol{r}\cdot\boldsymbol{u})]\\&=-\frac{u^2}{r}\frac{\boldsymbol{r}}{r}+\frac{u_\parallel}{r}\boldsymbol{u}.\end{aligned}$$

Hence, from (B 2)

$$\begin{aligned}\dot{\boldsymbol{\Omega}}\times\boldsymbol{r}&=\frac{1}{r^2}\left[(\boldsymbol{r}\times\boldsymbol{A})\times\boldsymbol{r}-2\frac{u_\parallel}{r}(\boldsymbol{r}\times\boldsymbol{u})\times\boldsymbol{r}\right]\\&=\frac{1}{r^2}\left[\boldsymbol{r}\times(\boldsymbol{A}\times\boldsymbol{r})-2\frac{u_\parallel}{r}\boldsymbol{r}\times(\boldsymbol{u}\times\boldsymbol{r})\right]\\&=\frac{1}{r^2}\left[\boldsymbol{A}\,r^2-\boldsymbol{r}\,(\boldsymbol{A}\cdot\boldsymbol{r})-2\frac{u_\parallel}{r}\boldsymbol{u}\,r^2+2\frac{u_\parallel}{r}\boldsymbol{r}\,(\boldsymbol{u}\cdot\boldsymbol{r})\right]\\&=\boldsymbol{A}-A_\parallel\frac{\boldsymbol{r}}{r}-2\frac{u_\parallel}{r}\boldsymbol{u}+2\frac{u_\parallel^2}{r}\frac{\boldsymbol{r}}{r}\\&=\boldsymbol{A}-A_\parallel\frac{\boldsymbol{r}}{r}-2\frac{u_\parallel}{r}\boldsymbol{u}+2\frac{u^2}{r}\frac{\boldsymbol{r}}{r}-2\frac{u_\perp^2}{r}\frac{\boldsymbol{r}}{r}\\&=\boldsymbol{A}-\left(A_\parallel+\frac{u_\perp^2}{r}\right)\frac{\boldsymbol{r}}{r}-\left(-\frac{u^2}{r}\frac{\boldsymbol{r}}{r}+\frac{u_\parallel}{r}\boldsymbol{u}\right)-\frac{u_\parallel}{r}\boldsymbol{u}+\frac{u^2}{r}\frac{\boldsymbol{r}}{r}-\frac{u_\perp^2}{r}\frac{\boldsymbol{r}}{r}\\&=\boldsymbol{A}-\left(A_\parallel\frac{\boldsymbol{r}}{r}+\frac{u_\perp^2}{r}\right)\frac{\boldsymbol{r}}{r}-\boldsymbol{\Omega}\times\boldsymbol{u}-\frac{u_\parallel}{r}\boldsymbol{u}+\frac{u_\parallel^2}{r}\frac{\boldsymbol{r}}{r}\\&=-\frac{u_\parallel}{r}\boldsymbol{u}+\frac{u_\parallel^2}{r}\frac{\boldsymbol{r}}{r}.\end{aligned}\tag{B 5}$$

Appendix C. Model performances in standard case studies

In order to analyse the model performances in situations independent of the DNS dataset by Biferale *et al.* (2005), the Richardson constant is computed for three standard case studies: (i) the case when the universal constant C_K assumes the literature value 2.1 (Sreenivasan 1995); (ii) when the values of the parameter pair $(\sigma_{1p}^2,\varepsilon)$, which are the one-point velocity variance and the turbulent kinetic energy dissipation, are taken equal to 1; and (iii) when the values of the pair (τ_L,λ), which are the Tennekes Lagrangian time scale (4.18) and the Eulerian length scale (5.22), are taken equal to 1.

The model is dependent on the parameter ρ (5.14), which is a function of C_K, C_0, $m_{4,0}$, $m_{2,2}$ and $m_{3,1}$ (5.15) and (5.16). This suggests that different values of the constant factors of the Eulerian statistics $m_{i,j}$ give a different determination of ρ. However, for the purpose of highlighting the dependence of the parameter ρ on C_K and C_0, the values of $m_{4,0}$, $m_{2,2}$ and $m_{3,1}$ given in (5.16) are preserved, then from (5.14) follows:

$$\rho=-\frac{659}{93}+\frac{16}{31}\frac{C_0}{C_K}.\tag{C 1}$$

https://doi.org/10.1017/S0022112008003820 Published online by Cambridge University Press

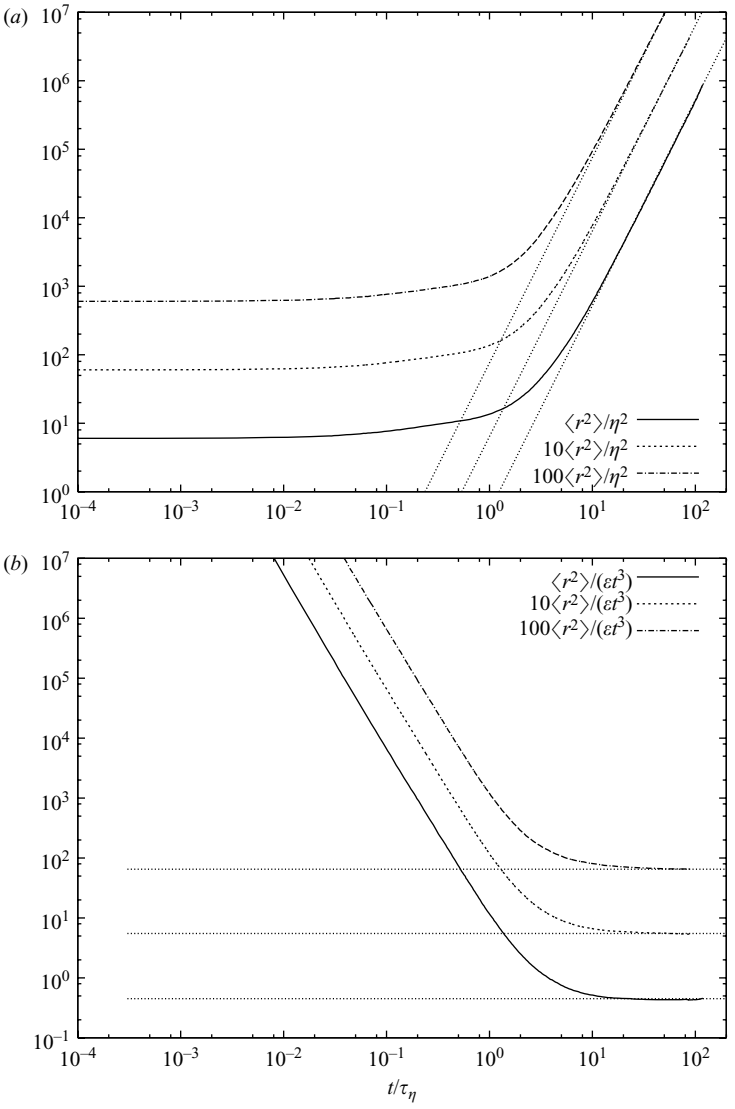


FIGURE 11. Plots of the variance of the particle separation $\langle r^2\rangle$ with $C_K = 2.1$ and $C_0 = 5$ (continuos line), $C_0 = 6$ (dotted line) and $C_0 = 7$ (dash-dotted line). The dotted straight lines are the fits with the corresponding Richardson constant: $g = 0.45$, 0.55 and 0.65.

The numerical simulations in the first case study are performed with 2000 particle pairs and the same conditions as in § 5.4.1. Moreover, they can be performed in two ways: first, with ρ determined as in (C 1) and second, with $\rho = -3653/651$ as in the rest of this paper. The plots of $\langle r^2\rangle$ for ρ determined as in (C 1), which are very similar to the case $\rho = -3653/651$, are shown in figure 11 for $C_0 = 5$, 6 and 7, respectively. The estimations of the Richardson constant turn out to be $g = 0.45$, 0.55 and 0.65, for the three values of $C_0 = 5$, 6 and 7, respectively.

For the other two case studies, the simulations are performed with 2000 particle pairs setting time step $\mathrm{d}t = 10^{-5}$, the initial separation $r_0 = 10^{-5}\lambda$, $C_K = 2$, $C_0 = 6$ and $\rho = -3653/651$. When $\sigma_{1p}^2 = \varepsilon = 1$, the Tennekes Lagrangian time scale (4.18)

https://doi.org/10.1017/S0022112008003820 Published online by Cambridge University Press

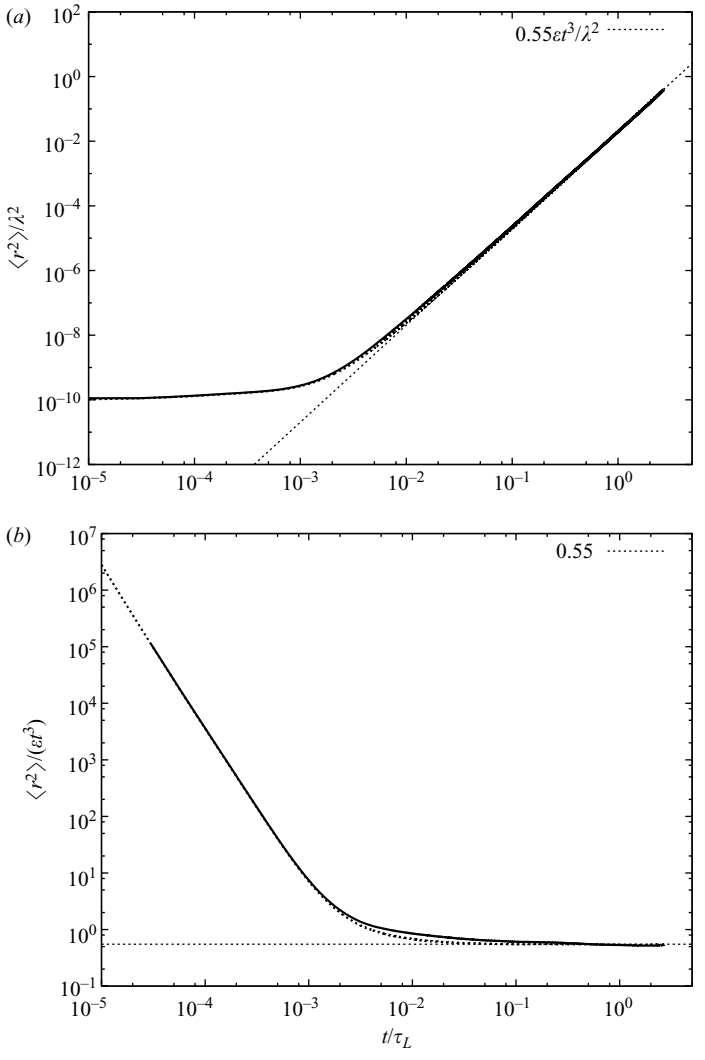


FIGURE 12. Plots of the variance of the particle separation $\langle r^2\rangle$ in the case studies $\sigma_{1p}^2 = \varepsilon = 1$ (continuos line) and $\tau_L = \lambda = 1$ (dotted line) with $C_K = 2$ and $C_0 = 6$. The dotted straight line is the fit with the Richardson constant: $g = 0.55$.

and the Eulerian length scale λ (5.22) are determined as

$$\tau_L = \frac{2\,\sigma_{1p}^2}{C_0\,\varepsilon} = \tfrac{1}{3}, \quad \lambda = \frac{1}{\varepsilon}\left(\frac{2\,\sigma_{1p}^2}{C_K}\right)^{3/2} = 1,$$

and when $\tau_L = \lambda = 1$ the parameters σ_{1p}^2 and ε are determined as

$$\sigma_{1p}^2 = \tfrac{1}{9}, \quad \varepsilon = \tfrac{1}{27}.$$

The results of these second and third case studies are shown in figure 12 and in both cases the Richardson constant turns out to be $g = 0.55$. These results are in very good

https://doi.org/10.1017/S0022112008003820 Published online by Cambridge University Press

agreement with the experimental value of the Richardson constant $g = 0.55 \pm 0.05$ (Berg *et al.* 2006) and the large-Reynolds-number limit estimation $g = 0.55 - 0.57$ by Sawford *et al.* (2008).

REFERENCES

Anfossi, D., Degrazia, G., Ferrero, E., Gryning, S. E., Morselli, M. G. & Trini Castelli, S. 2000 Estimation of the Lagrangian structure function constant C_0 from surface-layer wind data. *Boundary-Layer Met.* **95**, 249–270.

Anselmet, F., Antonia, R. A. & Danaila, L. 2001 Turbulent flows and intermittency in laboratory experiments. *Planet. Space Sci.* **49**, 1177–1191.

Antonia, R. A., Ould-Rouis, M., Zhu, Y. & Anselmet, F. 1997 Fourth-order moments of longitudinal- and transverse-velocity structure functions. *Europhys. Lett.* **37**, 85–90.

Antonia, R. A., Satyaprakash, B. R. & Chambers, A. J. 1982 Reynolds number dependence of velocity structure functions in turbulent shear flows. *Phys. Fluids* **25**, 29–37.

Batchelor, G. K. 1950 The application of the similarity theory of turbulence to atmospheric diffusion. *Q. J. R. Met. Soc.* **76**, 133–146.

Berg, J., Lüthi, B., Mann, J. & Ott, S. 2006 Backwards and forwards relative dispersion in turbulent flow: an experimental investigation. *Phys. Rev.* E **74**, 016304–1/7.

Biferale, L., Boffetta, G., Celani, A., Devenish, B. J., Lanotte, A. & Toschi, F. 2005 Lagrangian statistics of particle pairs in homogeneous isotropic turbulence. *Phys. Fluids* **17** (11), 115101–1/9.

Boffetta, G. & Sokolov, I. M. 2002 Relative dispersion in fully developed turbulence: the Richardson's law and intermittency corrections. *Phys. Rev. Lett.* **88** (9), 094501–1/4.

Borgas, M. S. & Sawford, B. L. 1991 The small-scale structure of acceleration correlations and its role in the statistical theory of turbulent dispersion. *J. Fluid Mech.* **228**, 295–320.

Borgas, M. S. & Sawford, B. L. 1994 A family of stochastic models for two-particle dispersion in isotropic homogeneous stationary turbulence. *J. Fluid Mech.* **279**, 69–99.

Borgas, M. S. & Yeung, P. K. 1998 Conditional fluid–particle accelerations in turbulence. *Theoret. Comput. Fluid Dyn.* **11**, 69–93.

Borgas, M. S. & Yeung, P. K. 2004 Relative dispersion in isotropic turbulence. Part 2. A new stochastic model with Reynolds-number dependence. *J. Fluid Mech.* **503**, 125–160.

Borgas, M. S., Flesch, T. K. & Sawford, B. L. 1997 Turbulent dispersion with broken reflectional symmetry. *J. Fluid Mech.* **332**, 141–156.

Du, S., Wilson, J. D. & Yee, E. 1994 On the moments approximation method for constructing a Lagrangian stochastic model. *Boundary-Layer Met.* **70**, 273–292.

Flesch, T. K. & Wilson, J. D. 1992 A two-dimensional trajectory-simulation model for non-Gaussian, inhomogeneous turbulence within plant canopies. *Boundary-Layer Met.* **61**, 349–374.

Franzese, P. & Borgas, M. S. 2002 A simple relative dispersion model for concentration fluctuations in contaminant clouds. *J. Appl. Met.* **41**, 1101–1111.

Franzese, P. & Cassiani, M. 2007 A statistical theory of turbulent relative dispersion. *J. Fluid Mech.* **571**, 391–417.

Frisch, U. 1996 *Turbulence. The Legacy of A. N. Kolmogorov*. Cambridge University Press.

Gardiner, C. W. 1990 *Handbook of Stochastic Methods for Physics, Chemistry and the Natural Sciences*, 2nd edn. Springer.

Heppe, B. M. O. 1998 Generalized Langevin equation for relative turbulent dispersion. *J. Fluid Mech.* **357**, 167–198.

Hill, R. J. 2002 Exact second-order structure–function relationships. *J. Fluid Mech.* **468**, 317–326.

Hill, R. J. & Boratav, O. N. 2001 Next-order structure–function equations. *Phys. Fluids* **13**, 276–283.

Hill, R. J. & Wilczak, J. M. 1995 Pressure structure functions and spectra for locally isotropic turbulence. *J. Fluid Mech.* **296**, 247–269.

Hill, R. J. & Wilczak, J. M. 2001 Fourth-order velocity statistics. *Fluid Dyn. Res.* **28**, 1–22.

Ishihara, T. & Kaneda, Y. 2002 Relative diffusion of a pair of fluid particles in the inertial subrange of turbulence. *Phys. Fluids* **14**, L69–L72.

https://doi.org/10.1017/S0022112008003820 Published online by Cambridge University Press

Kaplan, H. & Dinar, N. 1993 A three-dimensional model for calculating the concentration distribution in inhomogeneous turbulence. *Boundary-Layer Met*. **62**, 217–245.

Kurbanmuradov, O. A. 1997 Stochastic Lagrangian models for two-particle relative dispersion in high-Reynolds number turbulence. *Monte Carlo Meth. Applic*. **3**, 37–52.

Kurbanmuradov, O. A. & Sabelfeld, K. K. 1995 Stochastic Lagrangian models of relative dispersion of a pair of fluid particles in turbulent flows. *Monte Carlo Meth. Applic*. **1**, 101–136.

Kurbanmuradov, O. A., Sabelfeld, K. K. & Koluhin, D. 1997 Stochastic Lagrangian models for two-particle motion in turbulent flows. *Monte Carlo Meth. Applic*. **3**, 199–223.

Kurbanmuradov, O. A., Orszag, S. A., Sabelfeld, K. K. & Yeung, P. K. 2001 Analysis of relative dispersion of two particles by Lagrangian stochastic models and DNS methods. *Monte Carlo Meth. Applic*. **7**, 245–264.

Landau, L. D. & Lifshitz, E. M. 1960 *Mechanics*. Pergamon.

Li, Y. & Meneveau, C. 2005 Origin of non-Gaussian statistics in hydrodynamic turbulence. *Phys. Rev. Lett*. **95**, 164502–1/4.

Li, Y. & Menevau, C. 2006 Intermittency trends and Lagrangian evolution of non-Gaussian statistics in turbulent flow and scalar transport. *J. Fluid Mech*. **558**, 133–142.

Maurizi, A., Pagnini, G. & Tampieri, F. 2004 The dependence of relative dispersion on turbulence scales in Lagrangian stochastic models. *Phys. Rev*. E **69**, 037301–1/4.

Maurizi, A., Pagnini, G. & Tampieri, F. 2006 Turbulence scale dependece of the Richardson constant in Lagrangian stochastic models. *Boundary-Layer Met*. **118**, 55–68.

Monin, A. S. & Yaglom, A. M. 1971 *Statistical Fluid Mechanics,* vol. 1. MIT Press.

Monin, A. S. & Yaglom, A. M. 1975 *Statistical Fluid Mechanics,* vol. 2. MIT Press.

Monti, P. & Leuzzi, G. 1996 A closure to derive a three-dimensional well-mixed trajectory-model for non-Gaussian, inhomogeneous turbulence. *Boundary-Layer Met*. **80**, 311–331.

Narasimhan, M. N. L. 1993 *Principles of Continuum Mechanics*. John Wiley.

Nelkin, M. & Chen, S. 1998 The scaling of pressure in isotropic turbulence. *Phys. Fluids* **10**, 2119–2121.

Novikov, E. A. 1986 The Lagrangian–Eulerian probability relations and the random force method for nonhomogeneous turbulence. *Phys. Fluids* **29** (12), 3907–3909.

Novikov, E. A. 1989 Two-particle description of turbulence, Markov property, and intermittency. *Phys. Fluids* A **1** (2), 326–330.

Novikov, E. A. 1992 Probability distribution for three-dimensional vectors of velocity increments in turbulent flows. *Phys. Rev*. A **46**, R6147–R6149.

Obukhov, A. M. 1941 Energy distribution in the spectrum of turbulent flow. *Izv. Akad. Nauk. SSSR Geogr. Geofiz*. **5**, 453–466.

Ott, S. & Mann, J. 2000 An experimental investigation of the relative diffusion of particle pairs in three-dimensional turbulent flow. *J. Fluid Mech*. **422**, 207–223.

Ould-Rouis, M., Antonia, R. A., Zhu, Y. & Anselmet, F. 1996 Turbulent pressure structure function. *Phys. Rev. Lett*. **77**, 2222–2224.

Pagnini, G. 2005 Modelli stocastici per la dispersione turbolenta degli inquinanti nei fluidi geofisici. PhD thesis, University of Urbino.

Pearson, B. R. & Antonia, R. A. 2001 Reynolds-number dependence of turbulent velocity and pressure increments. *J. Fluid Mech*. **444**, 343–382.

Pedrizzetti, G. 1999 Quadratic Markov modeling for intermittent turbulence. *Phys. Fluids* **11** (6), 1694–1696.

Pedrizzetti, G. & Novikov, E. A. 1994 On Markov modelling of turbulence. *J. Fluid Mech*. **280**, 69–93.

Pope, S. 1985 PDF methods for turbulent reactive flows. *Prog. Energy Combust. Sci*. **11**, 119–192.

Praskovsky, A. & Oncley, S. 1994 Measurements of the Kolmogorov constant and intermittency exponent at very high Reynolds numbers. *Phys. Fluids* **6**, 2886–2888.

Reynolds, A. M. 1998 On trajectory curvature as a selection criterion for valid Lagrangian stochastic dispersion models. *Boundary-Layer Met*. **88**, 77–86.

Reynolds, A. M. 1999*a* On the non-uniqueness of Lagrangian stochastic models. *Fluid Dyn. Res*. **25**, 217–229.

Reynolds, A. M. 1999*b* The relative dispersion of particle pairs in stationary homogeneous turbulence. *J. Appl. Met*. **38**, 1384–1390.

https://doi.org/10.1017/S0022112008003820 Published online by Cambridge University Press

Reynolds, A. M. 2002 On the dynamical content of Lagrangian stochastic models in the well-mixed class. *Boundary-Layer Met.* **103**, 143–162.

Richardson, L. F. 1926 Atmospheric diffusion shown on a distance-neighbor graph. *Proc. R. Soc. Lond.* A **110**, 709–737.

Risken, H. 1989 *The Fokker–Planck Equation. Methods of Solution and Applications*, 2nd edn. Springer.

Sabelfeld, K. K. & Kurbanmuradov, O. A. 1997 Stochastic Lagrangian models for two-particle motion in turbulent flows. *Monte Carlo Meth. Applic.* **3**, 53–72.

Sabelfeld, K. K. & Kurbanmuradov, O. A. 1998 Two-particle stochastic Eulerian–Lagrangian models of turbulent dispersion. *Math. Comput. Simulation* **47**, 429–440.

Sawford, B. L. 1999 Rotation of trajectories in Lagrangian stochastic models of turbulent dispersion. *Boundary-Layer Met.* **93**, 411–424.

Sawford, B. L. 2001 Turbulent relative dispersion. *Annu. Rev. Fluid Mech.* **33**, 289–317.

Sawford, B. L. 2006 A study of the connection between exit-time statistics and relative dispersion using a simple Lagrangian stochastic model. *J. Turbulence* **7** (13), 1–10.

Sawford, B. L. & Borgas, M. S. 1994 On the continuity of stochastic models for the Lagrangian velocity in turbulent. *Physica* D **76**, 297–311.

Sawford, B. L. & Yeung, P. K. 2000 Eulerian acceleration statistics as a discriminator between Lagrangian stochastic models in uniform shear flow. *Phys. Fluids* **12** (8), 2033–424.

Sawford, B. L. & Yeung, P. K. 2001 Lagrangian statistics in uniform shear flow: direct numerical simulation and Lagrangian stochastic models. *Phys. Fluids* **13** (9), 2627–2634.

Sawford, B. L., Yeung, P. K. & Borgas, M. S. 2005 Comparison of backwards and forwards relative dispersion in turbulence. *Phys. Fluids* **17** (9), 095109–1/9.

Sawford, B. L., Yeung, P. K. & Hackl, J. F. 2008 Reynolds number dependence of relative dispersion statistics in isotropic turbulence. *Phys. Fluids* **20** (6), 065111–1/13.

She, Z. & Leveque, E. 1994 Universal scaling laws in fully developed turbulence. *Phys. Rev.* E **72**, 336–339.

Sneddon, I. N. 1972 *The Use of Integral Transform.* McGraw–Hill.

Sreenivasan, K. R. 1995 On the universality of the Kolmogorov constant. *Phys. Fluids* **7**, 2778–2784.

Sreenivasan, K. R. & Kailasnath, P. 1993 An update on the intermittency exponent in turbulence. *Phys. Fluids* A **5**, 512–514.

Tennekes, H. 1975 Eulerian–Lagrangian time microscales in isotropic turbulence. *J. Fluid Mech.* **67**, 561–567.

Tennekes, H. 1982 Similarity relations, scaling laws and spectral dynamics. In *Atmospheric Turbulence and Air Pollution Modeling* (ed. F. T. M. Nieuwstadt & H. van Dop), pp. 37–68. Reidel.

Tennekes, H. & Lumley, J. L. 1972 *A First Course in Turbulence.* MIT Press.

Thomson, D. J. 1987 Criteria for the selection of stochastic models of particle trajectories in turbulent flows. *J. Fluid Mech.* **180**, 529–556.

Thomson, D. J. 1990 A stochastic model for the motion of particle pairs in isotropic high-Reynolds-number turbulence, and its application to the problem of concentration variance. *J. Fluid Mech.* **210**, 113–153.

Wilson, J. D. & Flesch, T. K. 1997 Trajectory curvature as a selection criterion for valid Lagrangian stochastic models. *Boundary-Layer Met.* **84**, 411–425.

Yeung, P. K. & Borgas, M. S. 2004 Relative dispersion in isotropic turbulence. Part 1. Direct numerical simulations and Reynolds-number dependence. *J. Fluid Mech.* **503**, 93–124.

https://doi.org/10.1017/S0022112008003820 Published online by Cambridge University Press